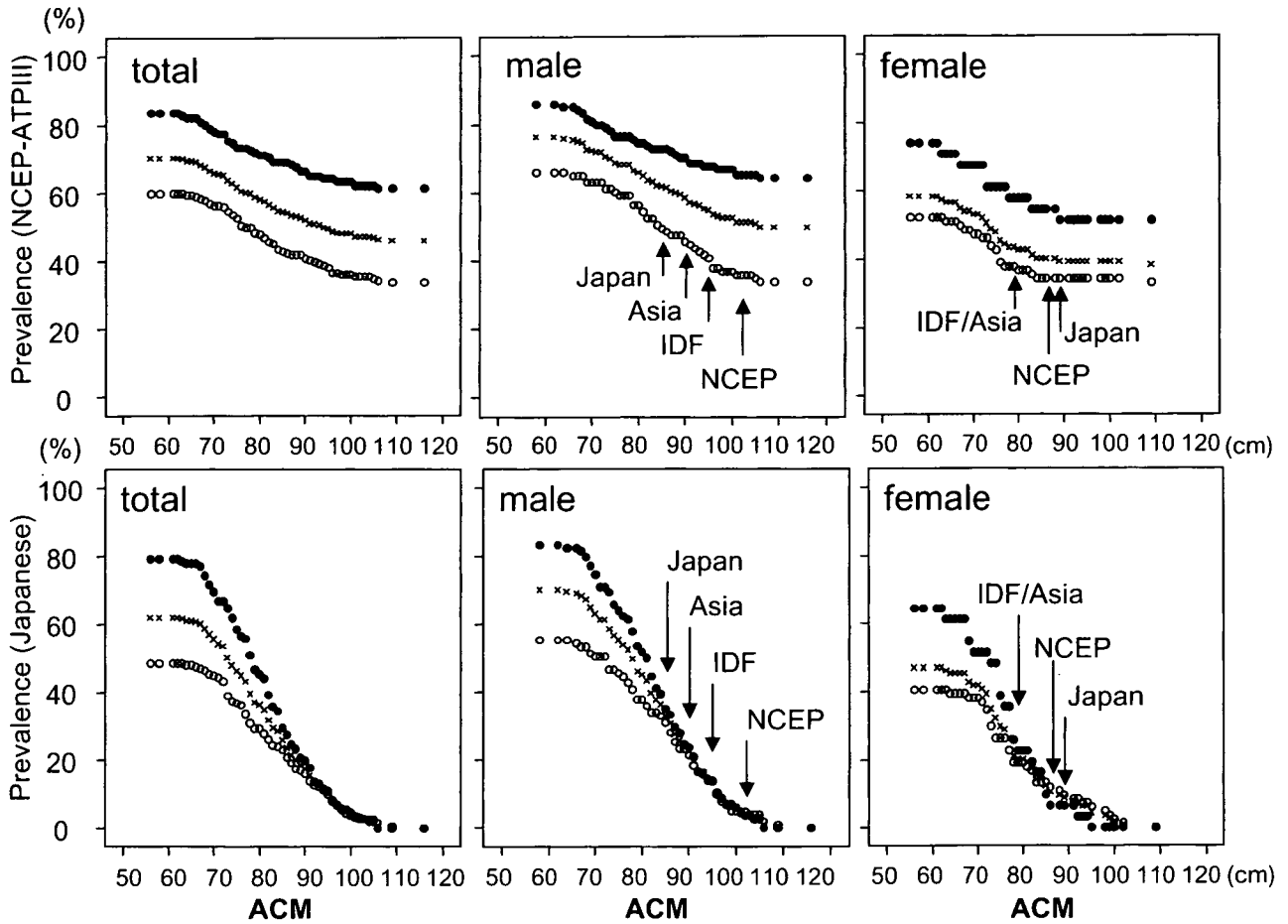

Fig. 7. *Relationship between the cutoff level of abdominal circumference and prevalence of metabolic syndrome. Upper: NCEP-ATP III–defined metabolic syndrome; Lower: metabolic syndrome defined by the current Japanese criteria. Open circles, closed circles and cross symbols represent relationships in subjects without ASCD, those with ASCD and all subjects, respectively.*

females. However, it has not been confirmed that the relationship between the level of VFA and the number of associated obesity-related diseases is quantitatively the same in both genders. Actually, a gender difference in the association of visceral fat accumulation with the other components of metabolic syndrome was recently reported by Miyawaki *et al.* (*13*) and was confirmed in the present study as well (Fig. 5). Miyawaki *et al.* (*13*) analyzed data from 3,574 Japanese subjects aged 40–59 years obtained during health examinations. The sensitivity and the specificity of VFA cutoff to predict metabolic syndrome were 0.72 and 0.55 at 95 cm^2 and 0.67 and 0.60 at 100 cm^2 in males, and the values in females were 0.73 and 0.70 at 65 cm^2 and 0.66 and 0.74 at 70 cm^2. These gender-dependent VFA cutoff levels are similar to those obtained in the present study (Fig. 5), indicating the need to define a VFA cutoff for each gender.

AC_M is a less accurate measure of visceral obesity than is VFA, but it is easier to use for screening of metabolic syndrome. Based on the VFA cutoff level for predicting metabolic syndrome in each gender and the regression equation for the VFA-AC_M relationship (Fig. 3), the AC_M cutoff levels for males and females were calculated in the present study to be 83 cm and 78 cm, respectively. Miyawaki *et al.* (*13*) calculated AC_M cutoff levels for males and females of 86 cm and 77 cm, respectively, based on their VFA cutoff levels of 100 cm^2 in males and 65 cm^2 in females. Although VFA was not determined in their study, Hara *et al.* (*14*) recently applied the waist circumference data for 692 subjects (age: 30–80 years) who had undergone annual health examinations to ROC analysis to determine the AC_M cutoff for diagnosis of metabolic syndrome. They found that the cutoff levels of AC_M yielding maximum sensitivity and specificity were 85 cm for males and 78 cm for females. The difference was partly due to the fact that they measured waist circumference at the mid-level between the lowest rib and the iliac crest, and that measurement in females is a few centimeters longer than AC_M (at the umbilicus level). Thus, Hara *et al.* (*14*) also estimated AC_M cutoff levels for males and females of ~85 cm and ~80 cm,

respectively. Taken together, the results of these two recent studies (*13*, *14*) and the results of the present study on Japanese subjects support the notion that the appropriate AC_M cutoff level for diagnosis of metabolic syndrome in Japanese females is 78–80 cm.

Prevalence of Metabolic Syndrome and Cutoff Level for Diagnosis of Visceral Obesity

To illustrate the effect of change in the cutoff level of visceral obesity on the prevalence of metabolic syndrome, we plotted the calculated prevalence of metabolic syndrome in the subjects for a range of AC_M cutoff levels (Fig. 7). The prevalence of NCEP-ATP III–defined metabolic syndrome was less sensitive to change in the AC_M cutoff level than was the prevalence of metabolic syndrome defined by the Japanese criteria, since visceral obesity is not a requisite in the former criteria. As shown in Fig. 7, the prevalences of NCEP-ATP III–defined metabolic syndrome in males were 51.0%, 59.2% and 62.0% for AC_M cutoff levels of 102 cm (NCEP-ATP III), 90 cm (IDF for Asians), and 85 cm (Japanese criteria). The prevalences were reduced to 35.9%, 47.6% and 50.5% when they were calculated for subjects without ASCD. The prevalences in females were 40.5%, 43.9% and 39.6% for AC_M cutoff levels of 88 cm (NCEP-ATP III), 80 cm (IDF for Asians) and 90 cm (Japanese criteria), respectively, and these values were reduced to 34.4%, 38.0% and 34.4%, respectively, when calculated for subjects without ASCD. In contrast, the prevalence of metabolic syndrome defined by the Japanese criteria is strongly dependent on AC_M cutoff levels: male AC_M cutoff levels of 102, 94, 90, and 85 cm give prevalences of metabolic syndrome of 4.6%, 16.0%, 23.8%, and 36.2%, and female AC_M cutoff levels of 88, 80, 90 and 78 cm give prevalences of 10.3%, 19.8%, 8.6% and 25.8%, respectively. Thus, the use of an AC_M cutoff level of 78 cm, which is suggested by the present results, triples the prevalence of metabolic syndrome in the present subjects.

In the recent Tanno-Soubetsu Study (*15*), the prevalence of metabolic syndrome as defined by the modified NECP-ATP III criteria (AC_M cutoff=85 cm) was 25.3% in 808 males undergoing health examinations, and their incidence of cardiovascular events was almost two-fold higher than that in subjects without metabolic syndrome (11.7% *vs.* 6.7%) during a 6-year follow up. The prevalence of metabolic syndrome in the present male subjects was approximately two-fold higher than that in the male subjects in the Tanno-Sobetsu Study, but this is likely to be due to selection bias in the present study. First, the subjects in the present study were older by 3 years (63±14 years old *vs.* 60±12 years old) and preferred in-hospital examination for ASCD and/or known coronary risks. Second, the proportion of subjects with ASCD was higher in this study than in the epidemiological studies. Nevertheless, the present study suggested that the prevalence of metabolic syndrome is lower in females than in males even when an AC_M cutoff of 78–80 cm was used for females. Whether metabolic syndrome in females has the impact on the cardiovascular events that it has in males will need to be investigated in large cohort studies.

Cutoff Level for Visceral Obesity and ASCD

Recent studies have shown that metabolic syndrome is associated with endothelial dysfunction (*16*), a hallmark of early atherosclerotic change, calcification of the coronary artery (*17*, *18*), and subclinical atherosclerosis of the carotid artery (*19*, *20*). On the other hand, obesity *per se* is an established risk factor of ASCD. Thus, we postulated that the AC_M cutoff to predict ASCD might be larger than that to predict metabolic syndrome, which consists of clustered minor risk factors. However, the AC_M cutoff level to predict metabolic syndrome and that to predict ASCD were very similar (Fig. 5B) in the present study. These results may suggest that the level of visceral obesity does not need to be higher than the level of obesity in metabolic syndrome in order for patients to develop ASCD. Nevertheless, the AC_M cutoff levels for diagnosis of metabolic syndrome appear to also be useful for selecting patients who should be screened for ASCD.

Limitations in the Present Study

There were several limitations in the present study. First, data collection was formed in a single institute by use of a retrospective and non-randomized method, which could have resulted in selection bias. Second, since this study is cross-sectional, a sequential relationship between visceral obesity and development of ASCD cannot be established. Third, a substantial number of the subjects were receiving treatment, including lifestyle modification and medications. Although the presence of diabetes mellitus does not preclude diagnosis of metabolic syndrome (*7–9*), it has profound effects on the metabolic profiles in patients. Furthermore, a recent Treating to New Targets (TNT) study (*21*) suggested that diabetes mellitus increases the incidence of cardiovascular events in patients with metabolic syndrome. Thus, it may be problematic to determine the VFA cutoff level for diagnosis of visceral obesity by use of mixed data from diabetic and non-diabetic populations. Fourth, we did not perform age-adjustment when calculating the AC_M cutoff, though there was a trend of age-dependent changes in VFA. Therefore, a further investigation using a large population with age-adjustment needs to be performed for obtaining a precise estimation of AC_M cutoff for diagnosis of metabolic syndrome in Japanese.

Acknowledgements

We would like to express special thanks to all the members of our department for discussion and comments on this study.

References

1. Castelli WP: Epidemiology of coronary heart disease: the Framingham study. *Am J Med* 1984; **76**: 4–12.
2. National Cholesterol Education Program: Summary of the second report of the National Cholesterol Education Program (NCEP) Expert Panel on Detection, Evaluation, and Treatment of High Blood Cholesterol in Adults (Adult Treatment Panel II). *JAMA* 1993; **269**: 3015–3023.
3. Reaven GM: Banting lecture 1988: role of insulin resistance in human disease. *Diabetes* 1988; **37**: 1595–1607.
4. Kaplan NM: The deadly quartet: upper-body obesity, glucose intolerance, hypertriglyceridemia, and hypertension. *Arch Intern Med* 1989; **149**: 1514–1520.
5. DeFronzo RA, Ferrannini E: Insulin resistance: a multifaceted syndrome responsible for NIDDM, obesity, hypertension, dyslipidemia, and atherosclerotic cardiovascular disease. *Diabetes Care* 1991; **14**: 173–194.
6. Fujioka S, Matsuzawa Y, Tokunaga K, Tarui S: Contribution of intra-abdominal fat accumulation to the impairment of glucose and lipid metabolism in human obesity. *Metabolism* 1987; **36**: 54–59.
7. Expert Panel on Detection, Evaluation and Treatment of High Blood Cholesterol in Adults: Executive Summary of the Third Report of the National Cholesterol Education Program (NCEP). Expert Panel on Detection, Evaluation and Treatment of High Blood Cholesterol in Adults (Adult Treatment Panel III). *JAMA* 2001; **285**: 2486–2497.
8. Alberti KG, Zimmet P, Shaw J: Metabolic syndrome—a new world-wide definition. A Consensus Statement from the International Diabetes Federation. *Diabet Med* 2006; **23**: 469–480.
9. Examination Committee of Criteria for 'Obesity Disease' in Japan: Japan Society for the Study of Obesity: New criteria for 'Obesity Disease' in Japan. *Circ J* 2002; **66**: 987–992.
10. Matsuzawa Y: Adipocytokines and metabolic syndrome. *Semin Vasc Med* 2005; **5**: 34–39.
11. Moller DE, Kaufman KD: Metabolic syndrome: a clinical and molecular perspective. *Annu Rev Med* 2005; **56**: 45–62.
12. Task Force for Japanese Metabolic Syndrome Criteria: Diagnostic criteria of metabolic syndrome in Japanese. *Nihon Naika Gakkai Zasshi* 2005; **94**: 794 (in Japanese).
13. Miyawaki T, Hirata M, Moriyama K, *et al*: Metabolic syndrome in Japanese diagnosed with visceral far measurement by computed tomography. *Proc Jpn Acad* 2005; **81**: 471–479.
14. Hara K, Matsushita Y, Horikoshi M, *et al*: A proposal for the cutoff point of waist circumference for the diagnosis of metabolic syndrome in the Japanese population. *Diabetes Care* 2006; **29**: 1123–1124.
15. Takeuchi H, Saitoh S, Takagi S, *et al*: Metabolic syndrome and cardiac disease in Japanese men: applicability of the concept of metabolic syndrome defined by the National Cholesterol Education Program–Adult Treatment Panel III to Japanese men—the Tanno and Sobetsu Study. *Hypertens Res* 2005; **28**: 203–208.
16. Quinones MJ, Hernandez-Pampaloni M, Schelbert H, *et al*: Coronary vasomotor abnormalities in insulin-resistant individuals. *Ann Intern Med* 2004; **140**: 700–708.
17. Hunt ME, O'Malley PG, Feuerstein I, Taylor AJ: The relationship between the 'metabolic score' and subclinical atherosclerosis detected with electron beam computed tomography. *Coron Art Dis* 2003; **14**: 317–322.
18. Wong ND, Sciammarella MG, Polk D, *et al*: The metabolic syndrome, diabetes, and subclinical atherosclerosis assessed by coronary calcium. *J Am Coll Cardiol* 2003; **41**: 1547–1553.
19. Tzou WS, Douglas PS, Srinivasan SR, *et al*: Increased subclinical atherosclerosis in young adults with metabolic syndrome: the Bogalusa Heart Study. *J Am Coll Cardiol* 2005; **46**: 457–463.
20. Hassinen M, Komulainen P, Lakka TA, *et al*: Metabolic syndrome and the progression of carotid intima-media thickness in elderly women. *Arch Intern Med* 2006; **166**: 444–449.
21. Deedwania P, Barter P, Carmena R, *et al*, Treating to New Targets Investigators: Reduction of low-density lipoprotein cholesterol in patients with coronary heart disease and metabolic syndrome: analysis of the Treating to New Targets study. *Lancet* 2006; **368**: 919–928.

Basic Res Cardiol 101:418–426 (2006)
DOI 10.1007/s00395-006-0595-2

ORIGINAL CONTRIBUTION

Activation of ERK and suppression of calcineurin are interacting mechanisms of cardioprotection afforded by δ-opioid receptor activation

Yoshihiro Ikeda
Tetsuji Miura
Jun Sakamoto
Takayuki Miki
Masaya Tanno
Hironori Kobayashi
Katsuhiko Ohori
Akari Takahashi
Kazuaki Shimamoto

Received: 13 November 2005
Returned for 1st revision: 12 December 2005
1st Revision received: 9 February 2006
Accepted: 7 March 2006
Published online: 17 April 2006

Y. Ikeda · T. Miura (✉) · J. Sakamoto · T. Miki · M. Tanno · H. Kobayashi · K. Ohori · A. Takahashi · K. Shimamoto
Second Department of Internal Medicine
Sapporo Medical University School of Medicine
South-1 West-16, Chuo-ku
Sapporo 060-8543, Japan
Tel.: +81-11/611-2111 ext. 3225
Fax: +81-11/644-7958
E-Mail: miura@sapmed.ac.jp

M. Tanno
Department of Pharmacology
Sapporo Medical University
School of Medicine
Sapporo, Japan

Abstract The aim of this study was to examine possible interactions of ERK and calcineurin in cardioprotection afforded by δ-opioid receptor stimulation. Infarction was induced in rat hearts by 20-min coronary occlusion and reperfusion. Tissue ERK level and calcineurin activity were determined by immunoblotting and an assay using a phosphopeptide substrate, respectively. Administration of a δ-opioid receptor agonist, D-Ala^2-D-Leu^5-enkephalin (DADLE, 1 mg/kg), before ischemia increased the phospho-ERK levels during ischemia and reduced infarct size (as percentage of risk area, %IS/RA) from 47.7 ± 2.3 % to 23.2 ± 2.5 %. This protection was abolished by 10 mg/kg of natrindole hydrochloride (NTI), a δ-opioid receptor antagonist. PD98059, a MEK1/2 inhibitor, abolished both ERK1/2 activation and infarct size limitation by DADLE. Calcineurin inhibitors, cyclosporine-A (5 mg/kg) and FK506 (3.5 mg/kg), reduced %IS/RA (27.4 ± 4.4 % and 29.9 ± 3.4 %, respectively). The protective effects of these calcineurin inhibitors were inhibited by PD98059, and the combination of DADLE with cyclosporine-A or FK506 did not afford further cardioprotection. DADLE significantly suppressed myocardial calcineurin activity, and this effect was inhibited by NTI. Suppression of calcineurin activity by FK506 was associated with modest activation of ERK1/2. These results suggest that suppression of calcineurin and activation of ERK1/2 are interacting mechanisms involved in cardioprotection by δ-opioid receptor activation.

Key words δ-opioid receptor – ERK – calcineurin – FK506 – infarct size

Introduction

The δ-opioid receptor is an important trigger in the mechanism of ischemic preconditioning [18, 25, 28], and activation of this receptor by its selective agonists affords significant cardioprotection comparable with that afforded by early or late preconditioning [4, 8, 10]. Investigations in the last decade have indicated the involvement of multiple signaling pathways mediated by protein kinases, including protein kinase C and extracellular signal-regulated kinase (ERK), in the mechanism of this δ-opioid receptor-induced cardioprotection [9–11, 18]. On the other hand, involvement of protein phosphatases in the cardioprotection afforded by δ-opioid receptor activation remains unclear. However, Lakshmikuttyamma et al. [15] recently reported that calcineurin activity was elevated after ischemia/reperfusion in the rat and human myocardium [4], and Sanna et al. [24] demonstrated interactions between calcineurin and ERK signaling pathways as regulatory mechanisms of cardiac gene regulation and growth. Whether such an interaction between protein phosphatases and protein kinases is operative in the mechanism of cardioprotection against infarction has not been examined.

In the present study, we examined the possibility that δ-opioid receptor activation suppresses calcineurin ac-

tivity, which modifies ERK-mediated protective signaling in cardiomyocytes. First, contribution of ERK to cardioprotection afforded by activated δ-opioid receptors and to protection afforded by calcineurin inhibitors was pharmacologically assessed by using infarct size as an end-point. In the second series of experiments, effects of δ-opioid receptor activation and calcineurin inhibition on levels of phospho-ERKs before and after ischemia were determined. In the last series of experiments, the effect of δ-opioid receptor activation on calcineurin activity in the myocardium was compared with that of FK506, a calcineurin inhibitor. The results support the notion that interaction of pathways mediated by ERKs and calcineurin contribute to the acquisition of anti-infarct tolerance in the myocardium after δ-opioid receptor activation.

Methods

This study was performed in strict accordance with the guidelines of the Committee for Animal Research, Sapporo Medical University.

Experiment I: Infarct Size Experiments

Surgical preparation

Male Sprague-Dawley rats weighing 280–390 g were prepared for induction of myocardial infarction as in our previous studies [20, 26, 28]. In brief, rats were anesthetized with sodium pentobarbital (40 mg/kg, i. p.), intubated, and mechanically ventilated with a Harvard rodent respirator (model 683, Harvard Apparatus, South Natick, MA, USA) with oxygen supplement. The heart of each rat was exposed via left thoracotomy and a snare was passed around the left main coronary. Saline-filled catheters were placed in the carotid artery and jugular vein for blood pressure monitoring and drug infusion, respectively. An electrocardiogram was recorded by bipolar electrodes on the chest. Rectal temperature was continuously monitored, and a heating lamp was used to maintain the temperature within the range of 37.5 to 38.5°C. After 20-min of a stabilization period, myocardial infarction was induced by 20-min coronary occlusion and reperfusion. Based on the results of our previous studies [20, 26, 28] in which the coronary artery was occluded for 20, 30 or 40 min to induce infarction, we selected 20-min ischemia in this study to induce necrosis in approximately 50% of the risk area in untreated controls. After 2 hr of reperfusion, rats were heparinized and sacrificed by pentobarbital overdose. Hearts were quickly excised for postmortem analysis.

Experimental protocol

Protocol 1: Rats were divided into 5 groups (Fig. 1A), and each group received no treatment (controls), D-Ala^2-D-Leu^5-enkephalin (DADLE, 1 mg/kg, i. v.) at 15 min before ischemia, DADLE at 5 min before reperfusion, PD98059 (2.5 mg/kg, i. v.), at 20 min before ischemia, or combination of PD98059 at 20 min before ischemia and DADLE at 15 min before ischemia.

Protocol 2: This series of experiments was performed to confirm that infarct size limitation by DADLE (see results) was mediated by the δ-opioid receptor. Rats were pretreated with a δ-opioid receptor antagonist, naltrindole hydrochloride (NTI, 10 mg/kg), or NTI and DADLE (1 mg/kg) (Fig. 1B). NTI was injected subcutaneously 35 min before ischemia and DADLE was injected intravenously 15 min before ischemia. This dose of NTI was selected on the basis of previous findings that 10 mg/kg of NTI abolished the infarct size-limiting effects of a δ-opioid agonist and ischemic preconditioning in rat hearts *in situ* [25, 28].

Protocol 3: Rats were divided into seven groups (Fig. 1C) and received no treatment, FK506 (3.5 mg/kg, i. v.), cyclosporine-A (5 mg/kg, i. v.), PD98059 (2.5 mg/kg, i. v.) and FK506, PD98059 and cyclosporine-A, FK506 and DADLE (1 mg/kg, i. v.), or cyclosporine-A

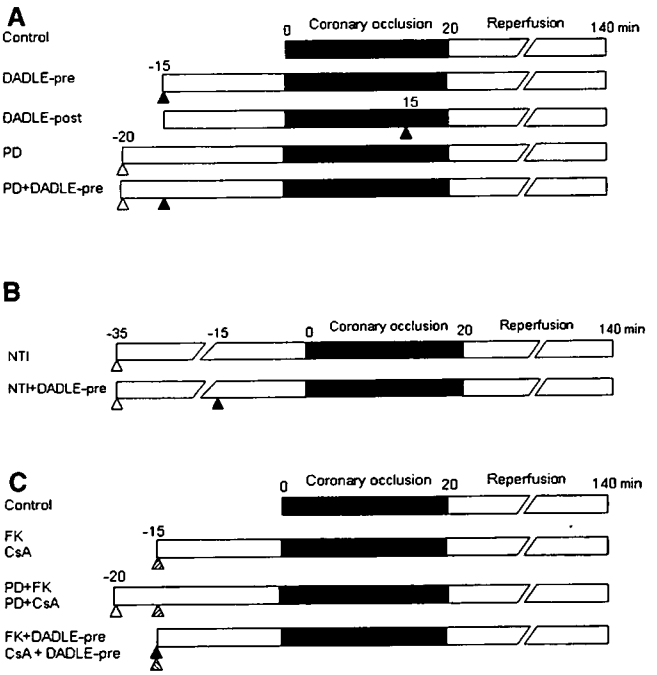

Fig. 1 Experimental protocols in infarct size experiments. **A–C** show protocol 1, protocol 2 and protocol 3, respectively. *PD* PD98059, *NTI* natrindole hydrochloride, *FK* FK506, *CsA* cyclosporin A. Solid arrowheads and open arrowheads indicate timings of DADLE injection and PD98059 injection, respectively. Hatched arrowheads indicate the timing of injection of calcineurin inhibitors (i. e., FK506 or cyclosporin A)

and DADLE. FK506, cyclosporine-A and DADLE were injected 15 min before ischemia. PD98050 was injected at 20 min before ischemia.

Postmortem analysis

Excised hearts were mounted onto a Langendorff apparatus, and after re-ligating the coronary artery, fluorescent polymer microspheres (Duke Scientific Co., Palo Alto, CA)suspended in saline were infused into the aorta to negatively mark the risk area. The heart was frozen and then sliced into 2-mm sections, and the sections were incubated with phosphate buffer containing 1% triphenyltetrazolium (pH 7.4) to visualize infarcts. Images of the risk areas and infarcted areas were taken under black light and room light, respectively, and sizes of these areas were determined by SigmaScan (SPSS, Chicago, IL). Volumes of infarct and risk area in each heart were calculated by multiplying size of each area by thickness of the heart slice.

☐ Experiment II: Immunoblot Experiments

Surgical preparation and protocol

Rats were anesthetized and ventilated as in Infarct Size Experiments.

Protocol 1: Rats received one of three pretreatments: no pretreatment, DADLE (1 mg/kg, i. v.) 15 min before ischemia or PD98059 (2.5 mg/kg) 20 min before ischemia and DADLE at 15 min before ischemia. In each treatment group, the heart was excised immediately before the onset of ischemia, at 5 min after ischemia, at 20 min after ischemia or at 5 min after reperfusion. Excised hearts were immediately soaked in ice-cold saline. Then Evans Blue dye was injected into the aorta to visualize the area at risk, and ventricular tissue in the risk area was quickly excised and frozen in liquid nitrogen.

Protocol 2: Rats received one of three pretreatments: no pretreatment, FK506 (3.5 mg/kg) 15 min before ischemia or PD98059 (2.5 mg/kg) 20 min before ischemia and FK506 15 min before ischemia. Hearts were excised immediately before the onset of ischemia or at 20 min after ischemia, and tissues in the risk area were frozen as were in Protocol 1.

Immunoblotting for ERKs

Immunoblotting was performed as in our previous studies [19–21]. In brief, frozen tissues (0.2–0.3 g) were homogenized in ice-cold lysis buffer (pH 7.5) containing 20 mM Tris, 150 mM NaCl, 1 mM Na_2EDTA, 1 mM EGTA, 1% Triton, 2.5 mM sodium pyrophosphate, 1 mM β-glycerophosphate, 1 mM Na_3VO_4, 1μg/ml leupeptine, 1 mM phenylmethylsulfonyl fluoride and protease cocktail (Complete Mini, Roche Diagnostics). The homogenate was centrifuged at 13,000 g for 15 min and the supernatant was used for electrophoresis. A Bio-Rad Protein Assay Kit (Bio-Rad, Hercules, CA) was used to determine protein concentration, and 40 mg of protein was electrophoresed on a 12.5% polyacrylamide gel. Proteins were blotted onto a PVDF membrane (Milipore, Bedford, MA), and after blocking with a Tris buffer containing 5% nonfat dry milk and 0.1% Tween 20, the blots were incubated with 1000-fold diluted antibodies against total ERK1/2 and phospho-ERK1/2 (Cell Signaling Technology, Beverly, MA). ERK and phospho-ERK were visualized by using an ECL Western blotting detection kit (Amersham, Buckinghamshire, UK) and quantified by densitometry using SigmaGel (SPSS, Chicago, IL).

☐ Experiment III: Tissue Calcineurin Experiments

Surgical preparation and protocols

Rats were anesthetized and ventilated as in Infarct Size Experiments, and the heart of each rat was exposed via left thoracotomy. In Protocol 1, rats were randomly divided into three groups and each group received intravenous injection of DADLE (1 mg/kg), FK506 (3.5 mg/kg) or no pretreatment 15 min before excision of the heart. Excised hearts were soaked and rinsed in ice-cold saline, and the left ventricular tissues were quickly sampled and frozen in liquid nitrogen. In Protocol 2, rats randomly received NTI (10 mg/kg) or NTI and DADLE (1 mg/kg). NTI was injected subcutaneously 35 min before tissue sampling and DADLE was injected intravenously 15 min before tissue sampling as in Protocol 1. In Protocol 3, rats received DADLE, FK506 or no pretreatment as in Protocol 1, and the coronary artery was occluded 15 min after each pretreatment. Hearts were excised at 20 min after coronary occlusion, and ventricular tissues in the risk area were sampled as in Experiment II.

Assay of calcineurin activity

Tissue calcineurin activity was determined according to the method described in earlier reports [5, 12] with slight modification. In brief, frozen tissues were homogenized in ice-cold lysis buffer as in Experiment II and centrifuged at 100,000 g for 45 min. The supernatant was diluted to 5 ng protein/ml and used for assay of calcineurin activity. Using a BIOMOL GREEN™ Calcineurin Assay Kit (AK-804), calcineurin phosphatase activity was determined by detecting phosphate released fromthe calcineurin-specific RIIphosphopeptide. Protein concentration was determined by using a Bio-Rad Protein Assay Kit.

Statistical Analysis

Results are presented as means ± standard error (SE). Differences in the hemodynamic parameters within and between study groups were analyzed by two-way repeated measures analysis of variance (ANOVA). Intergroup differences in infarct size data and immunoblot data were tested by one-way ANOVA. When overall ANOVA indicated a significant difference, multiple comparisons were conducted by Student-Newman-Keuls *post hoc* test. A p-value less than 0.05 was considered to be statistically significant.

Results

☐ Experiment I

Exclusion of rats

Ninety-two rats were used for Experiment I and 9 of those rats (2 control, 2 DADLE-treated, 1 NTI + DADLE-treated, 2 FK506-treated and 2 cyclosporine-A-treated rats) were excluded because of intractable ventricular fibrillation or hypotension during ischemia or reperfusion. There was no significant difference between incidences of exclusion in study groups.

Hemodynamic data

As shown in Table 1, heart rate and blood pressure levels are comparable in all study groups under baseline conditions, and there were no significant inter-group differences between these hemodynamic parameters in each protocol.

Infarct size data

Heart weight and the size of risk area were similar in all study groups (Table 2). In Protocol 1, DADLE injected before ischemia reduced infarct size as a percentage of risk area (%IS/RA) from 47.7 ± 2.3% in controls to 23.2 ± 2.5% (Fig. 2), and this protective effect was abrogated by PD98059 (%IS/RA = 43.5 ± 4.4%), while PD98059 alone did not modify %IS/RA (47.5 ± 5.4%). In contrast, DADLE administered 5 min before reperfusion failed to significantly reduce %IS/AR (40.1 ± 4.3%). In Protocol 2, infarct size-limiting effect of pretreatment with DADLE was not detected in NTI-treated rats (%IS/RA = 44.7 ± 5.4% vs. 46.3 ± 2.3%, p = NS). In Protocol 3, FK506 and cyclosporine-A similarly reduced %IS/RA from 45.0 ± 3.5% to 29.9 ± 3.4% and 27.4 ± 4.4%, respectively (Fig. 3). The combination of DADLE with FK506 or cyclosporine-A did not afford further cardioprotection (%IS/RA = 23.3 ± 3.5 and 27.5 ± 5%, both p = NS vs. FK506 alone and cyclosporine-A alone). PD98059 significantly attenuated the cardioprotection afforded by FK506

Table 1 Summary of hemodynamic parameters

Treatment	N	Heart Rate (beats per min)			Mean Blood Pressure (mmHg)		
		Baseline	Ischemia	Reperfusion	Baseline	Ischemia	Reperfusion
Protocol 1							
Control	7	424±16	415±18	409±8	91±3	78±7	96±6
DADLE-pre	7	436±15	429±14	423±15	102±6	103±6	101±12
DADLE-post	8	461±11	470±11	445±15	100±5	86±6	94±2
PD	6	463±6	450±11	447±14	101±6	86±8	87±2
PD + DADLE-pre	6	455±21	455±17	455±20	111±7	105±7	86±5
Protocol 2							
NTI	5	428±21	376±13	394±12	109±4	85±3	80±6
NTI + DADLE-pre	5	408±21	380±6	100±10	102±9	97±10	101±10
Protocol 3							
Control	8	417±12	428±17	419±7	91±6	85±9	94±6
FK	6	432±19	460±33	421±15	111±8	99±10	98±7
PD + FK	5	408±13	396±10	380±13	104±2	80±8	87±7
FK + DADLE-pre	5	398±12	414±14	418±5	106±8	86±12	99±8
CsA	5	435±10	435±11	415±14	102±7	87±4	101±8
PD + CsA	5	468±19	450±17	430±15	104±3	81±6	86±7
CsA + DADLE-pre	5	408±21	380±6	378±7	99±5	82±5	93±5

Mean ± SE
DADLE-pre DADLE before ischemia; *DADLE-post* DADLE after ischemia; *PD* PD98059, *NTI* natrindole hydrochloride; *FK* FK506; CsA cyclosporin A; *Ischemia* 10 min after ischemia; *Reperfusion* 60 min after reperfusion

Basic Research in Cardiology, Vol. 101, No. 5 (2006)

Table 2 Summary of infarct size data

Treatment	N	Heart Weight (g)	Area at Risk (cm^3)	Infarct Size (cm^3)	%IS/AR
Protocol 1					
Control	7	1.16±0.03	0.29±0.04	0.14±0.02	47.7±2.3
DADLE-pre	7	1.16±0.05	0.25±0.03	0.06±0.01*	23.2±2.5*
DADLE-post	8	1.29±0.04	0.30±0.04	0.13±0.02	40.1±4.3
PD	6	1.29±0.06	0.24±0.02	0.13±0.01	47.5±5.4
PD + DADLE-pre	6	1.32±0.05	0.28±0.02	0.14±0.02	43.5±4.4
Protocol 2					
NTI	5	1.57±0.07	0.22±0.02	0.10±0.01	46.3±2.3
NTI + DADLE-pre	5	1.53±0.10	0.31±0.02	0.14±0.02	44.7±5.4
Protocol 3					
Control	8	1.20±0.03	0.26±0.02	0.12±0.01	45.0±3.5
FK	6	1.30±0.05	0.23±0.02	0.07±0.01*	29.9±3.4*
PD + FK	5	1.23±0.05	0.30±0.02	0.12±0.01	40.5±2.4
FK + DADLE-pre	5	1.41±0.05	0.27±0.02	0.08±0.02*	23.3±3.5*
CsA	5	1.21±0.05	0.23±0.02	0.07±0.02*	27.4±4.4*
PD + CsA	5	1.36±0.04	0.22±0.02	0.11±0.01	46.6±3.5
CsA + DADLE-pre	5	1.30±0.05	0.29±0.03	0.10±0.01	27.5±5.0*

Mean ± SE
%IS/AR infarct size as a percentage of area at risk; *DADLE-pre* DADLE before ischemia; *DADLE-post* DADLE after ischemia; *PD* PD98059; *NTI* natrindole hydrochloride; *FK* FK506; *CsA* cyclosporin A. * $p < 0.05$ vs. Control

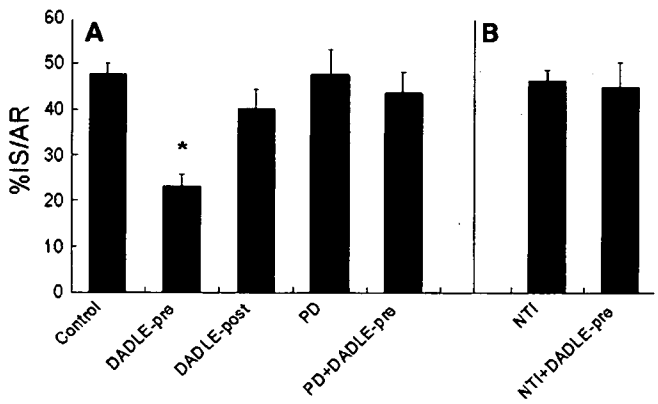

Fig. 2 Effects of DADLE on infarct size. **A** and **B** show data from protocol 1 and those from protocol 2, respectively. *%IS/AR* infarct size as a percentage of area at risk. *PD* PD98059, *NTI* natrindole hydrochloride. * $P < 0.05$ vs. Control

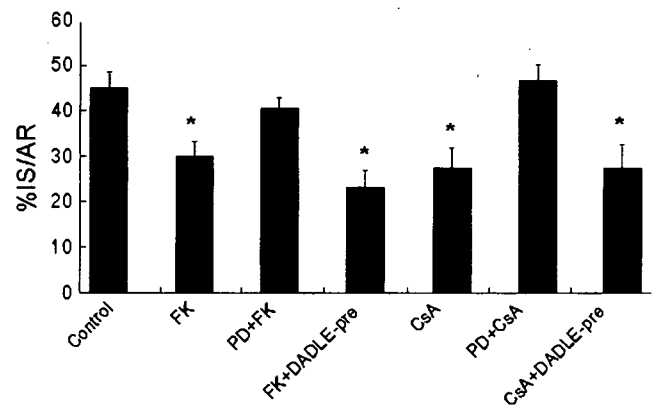

Fig. 3 Effects of calcineurin inhibitors on infarct size. *FK* FK506, *PD* PD98059, *CsA* cyclosporin A. *%IS/AR* infarct size as a percentage of area at risk. * $P < 0.05$ vs. Control

(%IS/RA = 40.5 ± 2.4 %) and that afforded by cyclosporine-A (%IS/AR = 46.6 ± 3.5 %).

☐ Experiment II

Ninety-six rats were used in this series of experiments and 6 of those rats were excluded because of intractable ventricular fibrillation or hypotension during ischemia. In Protocol 1, there was no significant difference in levels of total ERK1/2 before and after ischemia/reperfusion within and between study groups, and the levels of phospho-ERK1/2 before ischemia were similar in the study groups. Thus, levels of phospho-ERK1/2 after ischemia/reperfusion were expressed as percentage of each baseline level (Fig. 4). In controls, significant elevation of phospho-ERK1/2 levels was detected only after reperfusion. Administration of DADLE before ischemia significantly increased levels of phospho-ERK1/2 during ischemia, which was attenuated by PD98059. Neither DADLE nor PD98059 modified the increase in phospho-ERK1/2 after reperfusion. In Protocol 2 also, total ERK1/2 levels before and after ischemia were similar within and between study groups. FK506 alone did not change levels of phospho-ERK1/2 before ischemia but modestly increased levels of phospho-ERK1/2 20 min after ischemia (Fig. 5). However, this elevation of phospho-ERK1/2 levels was not inhibited by PD98059.

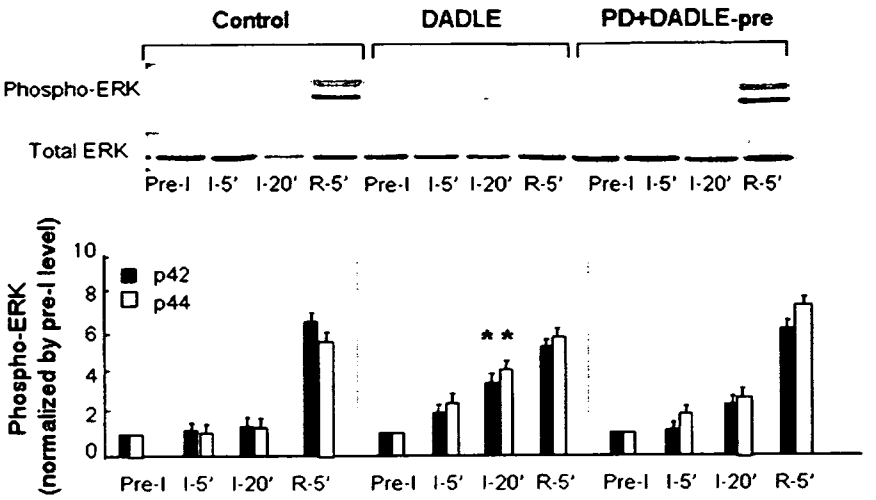

Fig. 4 Effects of DADLE on phospho-ERK levels in the myocardium before and after ischemia/reperfusion. *Pre-I* pre-ischemia, *I-5'* 5 min after ischemia, *I-20'* 20 min after ischemia, *R-5'* 5 min after reperfusion. Upper panels show representative immunoblots and lower panels show summarized data. * P < 0.05 vs. Pre-I level. N = 5~8 for each time point in each study group

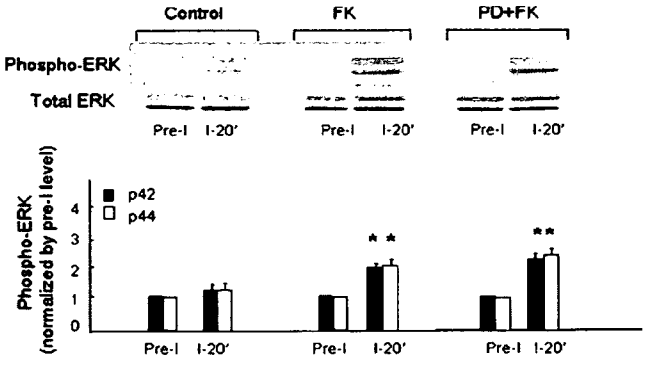

Fig. 5. Effects of FK506 on ERK level in the myocardium before and after ischemia. Pre-I = pre-ischemia, I-20' = 20 min after ischemia. Upper panels show representative immunoblots and lower panels show summarized data. *P < 0.05 vs. Pre-I level. N = 5~8 for each time point in each study group.

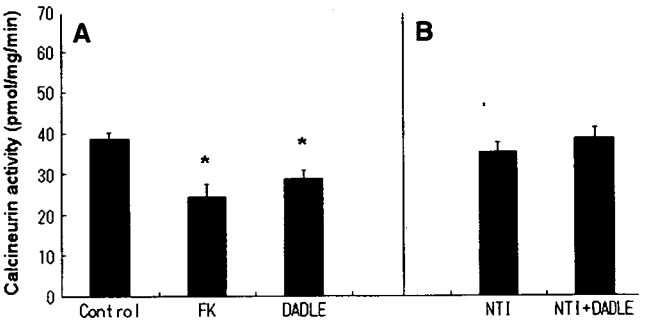

Fig. 6 Effects of FK506 and DADLE on calcineurin activity in the non-ischemic myocardium. **A** and **B** show data from protocol 1 and those from protocol 2, respectively. *FK* FK506, *NTI* natrindole hydrochloride. * P < 0.05 vs. Control. N = 8 in each study group of protocol 1, and n = 5 in each group of protocol 2

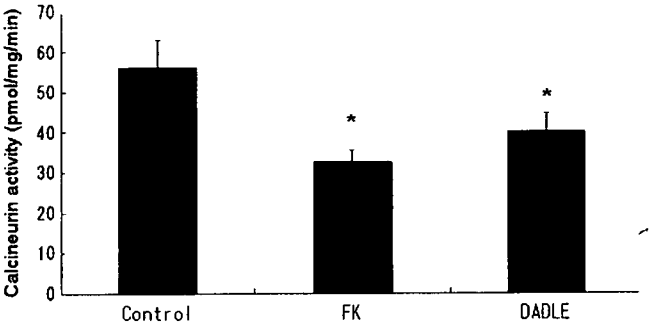

Fig. 7 Effects of pretreatments with FK506 and DADLE on myocardial calcineurin activity after 20-min ischemia. *FK* FK506. * P < 0.05 vs. Control. N = 5 in each study group

Experiment III

As shown in Fig. 6, calcineurin activity was significantly reduced by FK506 and also by DADLE in Protocol 1. There was no statistical difference between the calcineurin activities in DADLE-treated and FK506-treated hearts. In Protocol 2, calcineurin activity did not differ between hearts treated with NTI and hearts treated with NTI plus DADLE, and the levels of calcineurin activity were similar to the level in untreated controls of Protocol 1. The results of Protocol 3 indicate that FK506 and DADLE significantly reduced calcineurin activity in the ischemic myocardium (Fig. 7) as they did in the non-ischemic myocardium, though ischemia increased calcineurin activity by 1.5 fold in untreated hearts.

Discussion

Contribution of ERKs to cardioprotection afforded by δ-opioid receptor activation in rat hearts has been indicated by earlier findings that infarct size-limiting effects

of δ-opioid receptor agonists were abrogated by MEK1/2 inhibitors and that phosphorylation of ERK is induced by δ-opioid receptor agonists [9, 10]. However, the relationship between timing of ERK activation and augmentation of anti-infarct tolerance of the myocardium has been variously reported for different cardioprotective interventions in different models of myocardial infarction [3, 7, 9–11, 14, 23, 27]. In the present study, significant elevation of phospho-ERK1/2 levels by DADLE was detected during ischemia, and inhibition of ERK phosphorylation during the ischemic period by PD98059 (Fig. 4) was associated with loss of cardioprotection against infarction (Fig. 2). Furthermore, DADLE administered before reperfusion failed to limit infarct size. These results suggest that elevation of phospho-ERK level by activated δ-opioid receptors during ischemia is crucial for enhancement of myocardial tolerance against infarction. However, the period when up-regulated ERK during ischemia protects cardiomyocytes from necrosis may be at the time of reperfusion, since a close association of activated ERK upon reperfusion with cardioprotection has been shown by recent studies on preconditioning and post-conditioning [7, 14].

There are some apparent discrepancies between the effects of PD98059 on ERK phosphorylation and those on cardioprotection afforded by DADLE and FK506 in the present study. PD98059 failed to inhibit phosphorylation of ERK after reperfusion in DADLE-treated hearts, though this MEK inhibitor attenuated both DADLE-induced protection and ERK phosphorylation during ischemia. FK506-induced phosphorylation of ERK during ischemia was also unaffected by PD98059, whereas FK506-induced cardioprotection was inhibited by the same dose of PD98059. The reasons for these apparent discrepancies are not clear, but a few methodological problems may have been involved. First, ERK in several intracellular compartments is separately regulated [11, 23], which cannot be assessed from determination of phospho-ERK level in unfractionated tissue samples. Second, the effect of even a high dose of PD98059 (50 μM) can be overwhelmed when ERK is strongly activated by a large signal input from the activated receptors (i. e., large amount of agonist or expression of a large number of receptors) [2]. Third, MEK-independent mechanisms of ERK activation such as activation by protein kinase C (PKC) and phosphatidylinositol-3-kinase [13] were not examined in this study. Thus, inhibition of ERK relevant to cardioprotection by PD98059 could have been masked if ERK in intracellular compartments that were irrelevant to cytoprotection was phosphorylated by an overwhelmingly high level of activated MEK or by MEK-independent mechanisms.

Intracellular compartments in which activated ERK functions for myocyte protection have not been fully characterized. Fryer et al. [11] showed that the level of phospho-ERK in the cytosol but not that in the nucleus was associated with anti-infarct tolerance of the myocardium by ischemic preconditioning and a δ-opioid agonist. However, in a recent study by Reid et al. [23], infarct size limitation by adenosine receptor agonists was associated with elevation of phospho-ERK levels not only in cytosolic but also mitochondria and membrane fractions during both ischemia and reperfusion. Obviously further studies are necessary to clarify the role of activated ERK in each intracellular compartment during ischemia/reperfusion.

A role of protein phosphatase as a determinant of anti-ischemic tolerance of cells has been implicated by earlier findings that inhibitors of protein phosphatases protected the myocardium and brain from ischemic injury [1, 5, 6, 16, 17, 29, 30]. However, since those inhibitors are very different in terms of selectivity (to PP1, PP2A and PP2B and tyrosine protein phosphatase), it is difficult to identify a specific protein phosphatase relevant to protection of cells from ischemic injury. It has also not been known whether there is any endogenous mechanism regulating protein phosphatase activity for cell protection. The present study showed for the first time that activation of the δ-opioid receptor leads to suppression of calcineurin activity in the myocardium before and after the onset of ischemia (Figs. 6 and 7). Contribution of this suppression of calcineurin activity to infarct size-limiting effect of δ-opioid receptor activation is supported by two lines of circumstantial evidence. First, the level of suppression of tissue calcineurin activity by DADLE was comparable with that by FK506 (Fig. 6). Second, the same doses of DADLE and FK506 limited infarct size to equivalent levels, and the combination of DADLE with FK506 or another calcineurin inhibitor, cyclosporine-A, did not afford additive protection against infarction (Fig. 2 and Fig. 3).

The results of the present study are not sufficient to identify signaling steps in which inhibited calcineurin and activated ERK interact in cardiomyocytes. In the non-ischemic myocardium, FK506 significantly reduced calcineurin activity by approximately 40% but did not increase phospho-ERK levels, indicating that suppression of calcineurin activity *per se* does not trigger activation of ERK. On the other hand, phospho-ERK level after 20-min ischemia was elevated by FK506 (Fig. 5), which was associated with significant suppression of calcineurin activity (Fig. 7), and cardioprotection by FK506 was abrogated by PD98059 (Fig. 3). These findings suggest that ischemia-induced activation of ERK was augmented by suppression of calcineurin, leading to ERK-mediated cardioprotection. Although this notion is argued against by the findings that ERK phosphorylation during ischemia by FK506 was not inhibited by PD98059 (Fig. 5), the apparent contradiction may have been due to intracellular compartmentalization of ERK as discussed above. An alternative explanation, however,

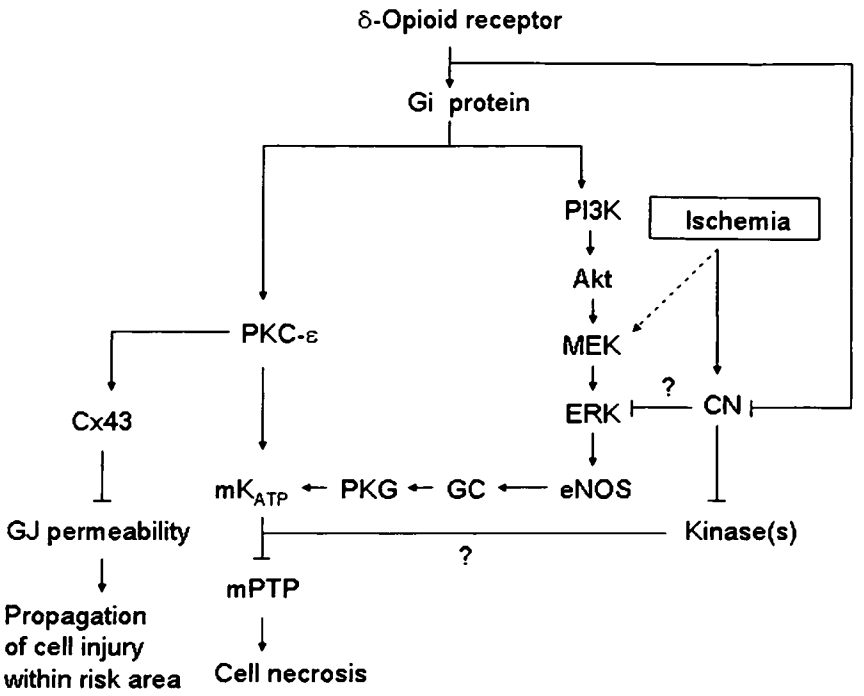

Fig. 8 Possible interactions between ERK and calcineurin in cardiomyocytes protection by δ-opioid receptor activation. Since infarct size-limiting effects of calcineurin (CN) inhibitors are sensitive to PD98059, a MEK1/2 inhibitor, there are two possible relationships between CN and ERK-mediated pathway. Inhibition of CN activity may induce myocyte protection by suppression of ischemia-induced ERK phosphorylation, which would consequently open the mitochondrial ATP sensitive potassium channel (mKATP). Alternatively, signal inputs from both the MEK-ERK pathway and a pathway augmented by calcineurin inhibition are required to activate downstream mechanisms such as suppression of the mitochondrial permeability transition pore (mPTP). Whether G proteins are involved in the suppression of CN by ∂-opioids and whether CN participates in regulation of connexin-43 (Cx43) phosphorylation remains to be investigated

is that a cell protective signaling pathway augmented by calcineurin inhibition and the MEK-ERK-mediated signaling pathway are in parallel, and inputs from these pathways are required to activate downstream mechanisms such as suppression of opening of the mitochondrial permeability transition pore. The possible relationships between calcineurin and ERK in the δ-opioid receptor-induced cardioprotection are shown in Fig. 8, which incorporates recent findings on the role of MEK/ERK activation in opening of the mitochondrial ATP-sensitive potassium channel [22] and our findings on the role of the gap junction downstream of PKC [19, 31]. Nevertheless, further investigation is necessary to clarify the interaction between calcineurin-mediated and ERK-mediated pathways in the cardioprotective mechanism.

As a limitation in the present study, it is unclear whether the relative importance of calcineurin suppression in the mechanisms of ∂-opioid receptor-induced cardioprotection is independent of duration of myocardial ischemia. DADLE significantly suppressed myocardial calcineurin activity before and after 20-min ischemia (Fig. 6 and Fig. 7), but the possibility that such an effect of DADLE is overcome by ischemia-induced elevation of calcineurin activity after a longer period of ischemia cannot be excluded.

In summary, the present study showed that interaction of activated ERK during ischemia and suppressed calcineurin is involved in the mechanism of anti-infarct tolerance of the myocardium afforded by δ-opioid receptor activation in rat hearts.

☐ **Acknowledgements** This study was supported by grant #08670812 from the Japan Society for the Promotion of Science, Tokyo, Japan and by a grant from Sapporo Medical University Academic Foundation, Sapporo, Japan.

References

1. Armstrong SC, Ganote CE (1992) Effects of the protein phosphatase inhibitors okadaic acid and calyculin A on metabolically inhibited and ischaemic isolated myocytes. J Mol Cell Cardiol 24:869–884
2. Aless DR, Cuenda A, Cohen P, Dudley, Saltiel AR (1995) PD098059 is a specific inhibitor of the activation of mitogen-activated protein kinase kinase in vitro and in vivo. J Biol Chem 270: 27489–27494
3. Behrends M, Schulz R, Post H, Alexandrov A, Belosjorow S, Michel MC, Heusch G (2000) Inconsistent relation of MAPK activation to infarct size reduction by ischemic preconditioning in pigs. Am J Physiol 279:H1111–H1119

4. Bell SP, Sack MN, Patel A, Opie LH, Yellon DM (2000) Delta opioid receptor stimulation mimics ischemic preconditioning in human heart muscle. J Am Coll Cardiol 36:2296–2302
5. Bueno OF, Wilkins BJ, Tymitz KM, Glascock BJ, Kimball TF, Lorenz JN, Molkentin JD (2002) Impaired cardiac hypertrophic response in Calcineurin Abeta-deficient mice. Proc Natl Acad Sci USA 99:4586–4591
6. Cai Q, Baxter GF, Yellon DM (1998) Reduction of infarct size in isolated rat heart by CsA and FK506: possible role of phosphatase inhibition. Cardiovasc Drugs Ther 12:499–501
7. Darling CE, Jiang R, Maynard M, Whittaker P, Vinten-Johansen J, Przyklenk K (2005) Postconditioning via stuttering reperfusion limits myocardial infarct size in rabbit hearts: role of ERK1/2. Am J Physiol 289:H1618–H1626
8. Fryer RM, Hsu AK, Gross GJ (2001) ERK and p38 MAP kinase activation are components of opioid-induced delayed cardioprotection. Basic Res Cardiol 96: 136–142
9. Fryer RM, Hsu AK, Eells JT, Nagase H, Gross GJ (1999) Opioid-induced second window of cardioprotection: potential role of mitochondrial K_{ATP} channels. Circ Res 84:846–851
10. Fryer RM, Wang Y, Hsu AK, Nagase H, Gross GJ (2001) Dependence of delta1-opioid receptor-induced cardioprotection on a tyrosine kinase-dependent but not a Src-dependent pathway. J Pharmacol Exp Ther 299:477–482
11. Fryer RM, Pratt PF, Hsu AK, Gross GJ (2001) Differential activation of extracellular signal regulated kinase isoforms in preconditioning and δpioid-induced cardioprotection. J Pharmacol Exp Ther 296:642–649
12. Goldspink PH, McKinney RD, Kimball VA, Geenen DL, Muttrick PM (2001) Angiotensin II induced cardiac hypertrophy in vivo is inhibited by cyclosporin A in adult rats. Mol Cell Biochem 226:83–88
13. Grammer TC, Blenis J (1997) Evidence for MEK-independent pathways regulating the prolonged activation of the ERK-MAP kinases. Oncogene 14: 1635–1642
14. Hausenloy DJ, Tsang A, Mocanu MM, Yellon DM (2005) Ischemic preconditioning protects by activating prosurvival kinases at reperfusion. Am J Physiol 288:H971–H976
15. Lakshmikuttyamma A, Selvakumar P, Kakkar R, Kanthan R, Wang R, Sharma RK (2003) Activation of calcineurin expression in ischemia-reperfused rat heart and in human ischemic myocardium. J Cell Biochem 90:987–997
16. Liem DA, Gho CC, Gho BC, Kazim S, Manintveld OC, Verdouw PD, Duncker DJ (2004) The tyrosine phosphatase inhibior bis(maltolato)-oxovanadium attenuates myocardial reperfusion injury by opening ATP-sensitive potassium channels. J Pharmacol Exp Ther 309: 1256–1262
17. Macleod MR, O'Collins T, Horky LL, Howells DW, Donnan GA (2005) Systematic review and metaanalysis of the efficacy of FK506 in experimental stroke. J Cereb Blood Flow Metab 25: 713–721
18. Miki T, Cohen MV, Downey JM (1998) Opioid receptor contributes to ischemic preconditioning through protein kinase C activation in rabbits. Mol Cell Biochem 186:3–12
19. Miura T, Ohnuma Y, Kuno A, Tanno M, Ichikawa Y, Nakamura Y, Yano T, Miki T, Sakamoto J, Shimamoto K (2004) Protective role of gap junctions in preconditioning against myocardial infarction. Am J Physiol 286:H214–H221
20. Nozawa Y, Miura T, Miki T, Ohnuma Y, Yano T, Shimamoto K (2003) Mitochondrial K_{ATP} channel-dependent and -independent phases of ischemic preconditioning against myocardial infarction in rat. Basic Res Cardiol 98:50–58
21. Ohnuma Y, Miura T, Miki T, Tanno M, Kuno A, Tsuchida A, Shimamoto K (2002) Opening of mitochondrial K_{ATP} channel occurs downstream of PKC-epsilon activation in the mechanism of preconditioning. Am J Physiol 283: H440–H447
22. Philipp S, Critz SD, Cui L, Solodushko V, Cohen MV, Downey JM. Localizing extracellular signal-regulated kinase (ERK) in pharmacological preconditioning's trigger pathway. Basic Res Cardiol 101:159–167; (Epub ahead of print)
23. Reid EA, Kristo G, Yoshimura Y, Ballard-Croft C, Keith BJ, Mentzer RM Jr, Lasley RD (2005) In vivo adenosine receptor preconditioning reduces myocardial infarct size via subcellular ERK signaling. Am J Physiol 288:H2253–H2259
24. Sanna B, Bueno OF, Dai Y-S, Wilkins BJ, Molkentin JD (2005) Direct and indirect interactions between calcineurin-NFAT and MEK1-extracellular signal-regulated kinase 1/2 signaling pathways regulate cardiac gene expression and cellular growth. Mol Cell Biol 25: 865–878
25. Schultz JJ, Hsu AK, Gross GJ (1997) Ischemic preconditioning and morphine-induced cardioprotection involve the delta-opioid receptor in the intact rat heart. J Mol Cell Cardiol 29:2187–2195
26. Tanno M, Tsuchida A, Nozawa Y, Matsumoto T, Hasegawa T, Miura T, Shimamoto K (2000) Roles of tyrosine kinase and protein kinase C in infarct size limitation by repetitive ischemic preconditioning in the rat. J Cardiovasc Pharmacol 35:345–352
27. Toma O, Weber NC, Wolter JI, Obal D, Preckel B, Schlack W (2004) Desflurane preconditioning induces time-dependent activation of protein kinase C epsilon and extracellular signal-regulated kinase 1 and 2 in the rat heart in vivo. Anesthesiology 101:1372–1380
28. Tsuchida A, Miura T, Tanno M, Nozawa Y, Kita H, Shimamoto K (1998) Time window for the contribution of the delta-opioid receptor to cardioprotection by ischemic preconditioning in the rat heart. Cardiovasc Drugs Ther 12: 365–373
29. Weinbrenner C, Baines CP, Liu G-S, Armstrong SC, Ganote CE, Walsh AH, Honkanen RE, Cohen MV, Downey JM (1998) Fostriecin, an inhibitor of protein phosphatase 2A, limits myocardial infarct size even when administered after onset of ischemia. Circulation 98: 899–905
30. Weinbrenner C, Liu G-S, Downey JM, Cohen MV (1998) Cyclosporine A limits myocardial infarct size even when administered after onset of ischemia. Cardiovasc Res 38:676–684
31. Yano T, Miki T, Sakamoto J, Nakamura Y, Kobayashi H, Ikeda Y, Nishihara M, Miura T (2004) Activation of the ∂-opioid receptor induces phosphorylation of Ser368 in connexin43 by PKC-ε in the myocardium and enhances its tolerance against infarction. (Abstract) Circulation 110 (Suppl. III):137

EMBO
reports

scientific report

Ligand-independent activation of vascular endothelial growth factor receptor 1 by low-density lipoprotein

Ryosuke Usui[1], *Masabumi Shibuya*[2], *Shun Ishibashi*[3] & *Yoshiro Maru*[1,4+]

[1]Department of Pharmacology, Tokyo Women's Medical University, Shinjuku-ku, Tokyo, Japan, [2]Department of Genetics, Institute of Medical Science, University of Tokyo, Minato-ku, Tokyo, Japan, [3]Division of Endocrinology and Metabolism, Department of Internal Medicine, Jichi Medical University, Shimotsuke, Tochigi, Japan, and [4]IREIIMS, Tokyo Women's Medical University, Shinjuku-ku, Tokyo, Japan

Elevated serum low-density lipoprotein (LDL) is a risk factor for atherosclerotic disorders. However, prominent atherosclerosis, which has been observed in LDL receptor (LDLR)-knockout mice, has diminished the significance of LDLR as a cause of atherosclerosis, while elaborate studies have focused on the receptors for denatured LDL. Here we report that native LDL (nLDL) activates vascular endothelial growth factor (VEGF) receptor 1 (VEGFR1) but not VEGFR2 through LDLR and is as potent as VEGF in macrophage migration. Binding and co-endocytosis of VEGFR1 and LDLR were enhanced by nLDL, which is concomitant with ubiquitination-mediated degradation of VEGFR1. We propose that LDLR-mediated use of VEGFR1 by nLDL could be a potential therapeutic target in atherosclerotic disorders.

Keywords: VEGF receptor 1; LDL receptor; macrophage migration; atherosclerosis

EMBO reports (2007) 8, 1155–1161. doi:10.1038/sj.embor.7401103

INTRODUCTION

Accumulating evidence indicates that serum low-density lipoprotein (LDL) is a crucial risk factor for atherosclerotic cardiovascular disorders. Therapeutic reduction in the serum LDL level can suppress the onset and recurrence of these disorders, and eventually decrease the mortality rate (Baigent *et al*, 2005). Mutations in the native LDL (nLDL) receptor (LDLR) have been reported in familial hypercholesterolaemia (Brown & Goldstein, 1986). Interestingly, however, in both familial hypercholesterolaemia patients and LDLR-knockout mice (Ishibashi *et al*, 1994), paradoxical progression of atherosclerosis has been observed, suggesting the possible existence of other functional receptors for LDL. Receptors for modified versions of LDL such as oxidized LDL, which include the scavenger receptors (SR)-A, CD36 and FcγRII-B2, have been extensively studied (Moore & Freeman, 2006). Macrophages in the atherosclerotic plaque are morphologically and functionally transformed by oxidized LDL but not nLDL (Steinberg *et al*, 1989). However, nLDL induces macrophage migration by unknown mechanisms (Hara *et al*, 1992), whereas little attention has been paid to LDLR.

Microvessels in atherosclerotic plaques greatly contribute to the progression and stability of atherosclerosis (Moulton *et al*, 2003). It is well known that vascular endothelial growth factor (VEGF) has a central role in promoting vascularization. VEGF has two specific receptors, VEGFR1 and VEGFR2, with tyrosine kinase activity. Both are expressed in endothelial cells, VEGFR2 exclusively but VEGFR1 is also exceptionally expressed in macrophages (Shibuya, 2006). It has been reported that VEGFR1 antibody has an inhibitory effect on atherosclerotic plaque formation in apoE$^{-/-}$ hypercholesterolaemic mice, suggesting that VEGFR1 promotes atherosclerosis (Luttun *et al*, 2002).

Here, we report a previously unrecognized linkage between LDLR and VEGFR1.

RESULTS

Native LDL induces VEGFR1 endocytosis

Because of sterol-mediated transcriptional downregulation, LDLR is thought to be upregulated by lipoprotein-deficient serum (LPDS) or serum starvation (Brown & Goldstein, 1986). We found that LDLR was expressed in a variety of cells when deprived of serum (Fig 1A; supplementary Fig 1A online). When nLDL labelled with DiI (1,1′-dioctadecyl-3,3,3′,3′ -tetramethylindocarbocyanine perchlorate) was applied to 293T cells transiently transfected with VEGFR1 tagged with green fluorescent protein (GFP; VEGFR1-GFP) and subsequently starved of serum for 8 h, VEGFR1 was internalized and colocalized with DiI-nLDL in a VEGF-independent manner (Fig 1B,C). A similar phenomenon was observed in RAW cells (Fig 1B,C), a macrophage cell line that has been shown to

[1]Department of Pharmacology, Tokyo Women's Medical University, 8-1 Kawada-cho, Shinjuku-ku, Tokyo 162-8666, Japan
[2]Department of Genetics, Institute of Medical Science, University of Tokyo, 4-6-1 Shirokanedai, Minato-ku, Tokyo 108-8639, Japan
[3]Division of Endocrinology and Metabolism, Department of Internal Medicine, Jichi Medical University, 3311-1 Yakushiji, Shimotsuke, Tochigi 329-0498, Japan
[4]IREIIMS, Tokyo Women's Medical University, 8-1 Kawada-cho, Shinjuku-ku, Tokyo 162-8666, Japan
+Corresponding author. Tel: +81 3 5269 7417; Fax: +81 3 5269 7417;
E-mail: ymaru@research.twmu.ac.jp

Received 20 February 2007; revised 10 September 2007; accepted 11 September 2007; published online 26 October 2007

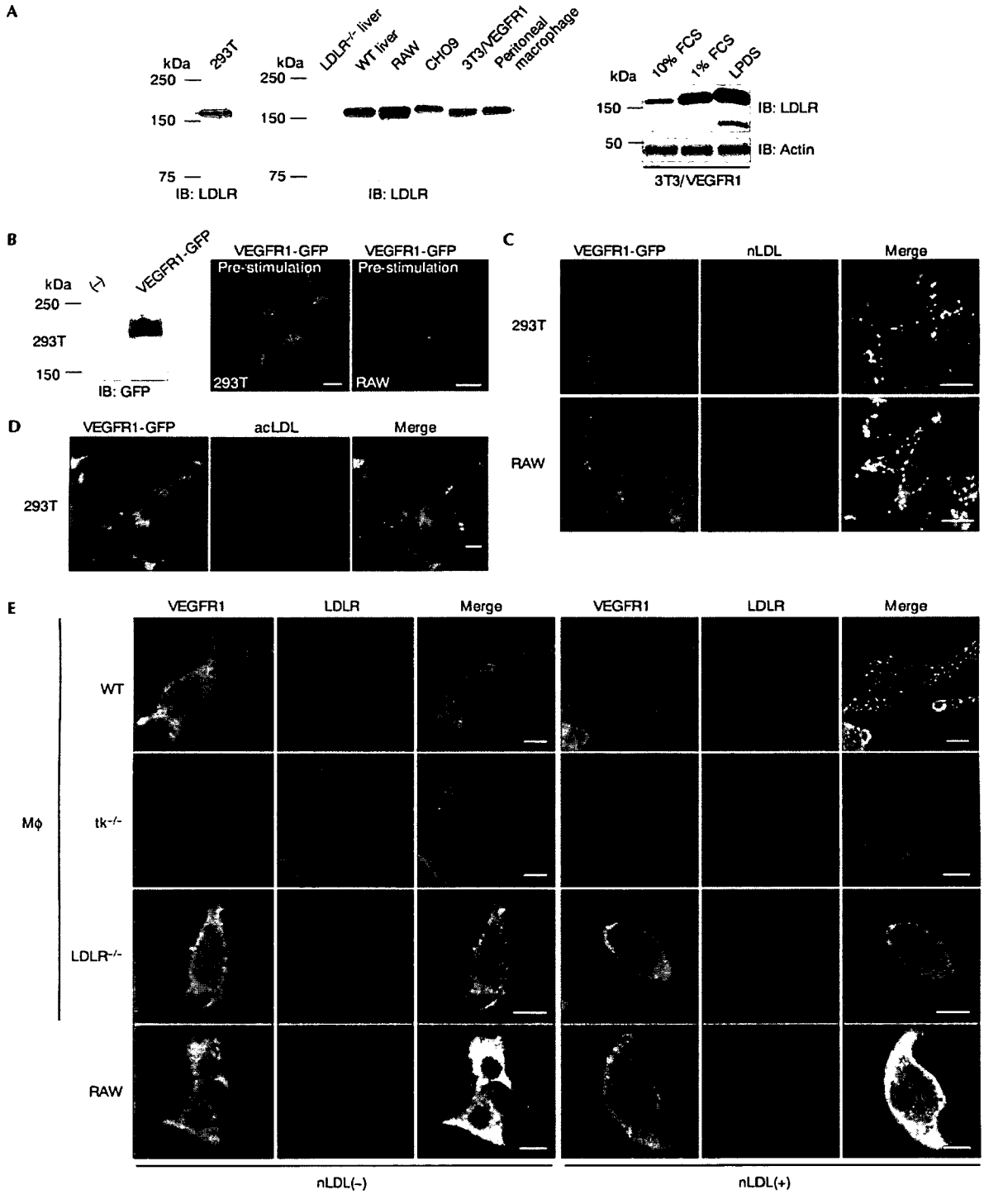

express endogenous VEGFR1 (Matsumoto *et al*, 2002). The concentration of nLDL that gave a significant number of VEGFR1-GFP endocytic vesicles was at least 10 μg/ml, which was comparable with that of VEGF on a molar basis in the same assay (Crouse *et al*, 1985; Kobayashi *et al*, 2004; supplementary Fig 1B online, also see legend). Interestingly, denatured LDL such as acetylated LDL (DiI-acLDL) failed to induce VEGFR1 endocytosis (Fig 1D). Given that acLDL uses receptors that cannot

Fig 1 | Native low-density lipoprotein induces endocytosis of VEGFR1. (A) Immunoblotting (IB) of whole-cell lysates (WCLs; 30 μg each) from human 293T cells (left) with human LDLR antibody and those from rodent cells with mouse LDLR antibody, including the liver of LDLR $^{-/-}$ and WT mice, RAW, CHO9, NIH3T3 cells overexpressing VEGFR1 (3T3/VEGFR1) and peritoneal macrophages (middle). Cell lines were cultured in 1% FCS for 24 h before protein extraction. WCLs from 3T3/VEGFR1 cultured in 10% and 1% serum, or LPDS were also subjected to anti-LDLR and anti-actin immunoblotting (right). **(B)** WCLs of 293T cells transfected with the VEGFR1-GFP expression vector or mock (−) were immunoblotted with GFP antibody (left). Membrane localization of VEGFR1-GFP transfected into 293T or RAW cells before nLDL stimulation (right). Scale bars, 10 μm. **(C,D)** 293T or RAW cells transfected with VEGFR1-GFP (green) were incubated with 10 μg/ml DiI-nLDL (red) **(C)** or 10 μg/ml DiI-acLDL (red) **(D)** for 30 min. Note the merged images with nLDL but not acLDL. Scale bars, 10 μm. **(E)** Peritoneal macrophages (MΦ) derived from WT, tk $^{-/-}$, LDLR $^{-/-}$ and RAW cells were immunostained with VEGFR1 and LDLR antibodies before (−) and after (+) stimulation by nLDL at 100 μg/ml. acLDL, acetylated LDL; GFP, green fluorescent protein; LDL, low-density lipoprotein; LDLR, LDL receptor; LPDS, lipoprotein-deficient serum; nLDL, native LDL; VEGFR, vascular endothelial growth factor receptor; WT, wild type.

bind to LDL, we suppose that nLDL could stimulate specific co-endocytosis of its own receptor LDLR and VEGFR1.

Native LDL stimulates recruitment of VEGFR1 to LDLR

Transient co-transfection of CHO9 cells with VEGFR1-GFP and LDLR tagged with Flag (LDLR-Flag) showed nLDL-stimulated endocytosis and colocalization of both receptors (supplementary Fig 1C,D online). This was blocked by SU5416, a VEGFR tyrosine kinase inhibitor. VEGF induced endocytosis of VEGFR1, but not LDLR, suggesting that the co-endocytosis is governed by nLDL and is VEGFR1-dependent. Clathrin has been shown to mediate LDLR endocytosis (Brown & Goldstein, 1986). However, we repeatedly failed to show nLDL-stimulated colocalization of VEGFR1 and clathrin (supplementary Fig 2A online). These results indicate a clathrin-independent pathway for LDLR endocytosis.

We established a RAW cell line that stably overexpressed the Flag-tagged human LDLR (RAW/LDLR-Flag). Stimulation by nLDL changed its subcellular localization from the membrane to the internalized vesicles (supplementary Fig 2B online). We also observed that some of the cells showed endocytic vesicles even before nLDL stimulation (data not shown). VEGFR1 was detected in the anti-Flag immunoprecipitates from RAW/LDLR-Flag cells. We pulled down VEGFR1 by using the ability of VEGFR1 to bind efficiently to a heparin column and used the heparin-bound VEGFR1 as a size control.

To test whether the co-endocytosis of LDLR and VEGFR1 is dependent on LDLR, we transiently transfected VEGFR1-GFP into skin fibroblasts derived from wild-type or LDLR$^{-/-}$ mice (Ishibashi *et al*, 1994) and stimulated them with nLDL. As shown in supplementary Figure 2C online, endocytosis was observed in wild-type but not LDLR$^{-/-}$ cells. We further examined the co-endocytosis of endogenous LDLR and VEGFR1 in RAW cells and peritoneal macrophages derived from wild-type, LDLR$^{-/-}$ and tk$^{-/-}$ mice (Hiratsuka *et al*, 1998), in which the intracellular domain of VEGFR1 was genetically deleted (Fig 1E). Consistent with the results shown above, we found that co-endocytosis is dependent on both LDLR and the VEGFR1 tyrosine kinase domain.

Binding of endogenous LDLR to VEGFR1 in the anti-VEGFR1 immunoprecipitates from RAW cells was detected and increased 3.5-fold (average of three independent experiments) with nLDL stimulation (Fig 2A). To test whether VEGFR1 in endothelial cells also interacts with LDLR, we stimulated human umbilical vein endothelial cells with nLDL. Enhanced binding between the receptors was observed (Fig 2B). To confirm further the interaction between the two receptors of endogenous origin, we immunoprecipitated VEGFR1 from the whole mouse lung, as the lung is one of the organs that express VEGFR1 most abundantly (Shibuya, 2006). The antibody used for immunoprecipitation recognizes only the intracellular domain of VEGFR1. The immunoprecipitates contained endogenous LDLR when the lung was derived from wild-type but not tk$^{-/-}$ mice (Fig 2C). This indicates that the interaction is specific, and the observed band is not a non-specifically precipitated LDLR. To test whether the binding between LDLR and VEGFR1 is mediated by the intracellular or extracellular portion of each receptor, we tried another antibody that recognizes only the extracellular domain of VEGFR1. As LDLR was immunoprecipitated with VEGFR1 in both wild-type and tk$^{-/-}$ cells with a similar efficiency, we assume that the binding might be mediated by the extracellular domains (Fig 2D). In both VEGFR1 antibodies, the immunoprecipitates did not contain nonspecific membrane proteins such as epidermal growth factor receptor (EGFR) or platelet-derived growth factor receptor; (PDGFR; Fig 2C,D).

Native LDL induces VEGFR1 autophosphorylation

As cells that express VEGFR1 at levels high enough for experimentally controlled molecular analysis are unavailable, we used NIH3T3 cells that stably overexpressed VEGFR1 (3T3/VEGFR1) and that were previously shown to have VEGF-dependent endocytosis of VEGFR1 (Kobayashi *et al*, 2004). We initially confirmed that endocytosis of LDLR takes place in these cells by an ^{125}I-LDL internalization assay, as shown in supplementary Fig 3 online. Both nLDL and VEGF induced degradation of VEGFR1 (by 45% and 50% within 20 min, respectively) but not LDLR in a time-dependent manner (supplementary Fig 4A,B online). As ErbB2 receptor tyrosine kinase was internalized and degraded by heat-shock protein 90 (Hsp90) inhibitor geldanamycin (Lerdrup *et al*, 2006), we examined the effects of the Hsp90 inhibitors on VEGFR1 (supplementary Fig 5A–D online). The inhibitors induced time-dependent degradation of VEGFR1 by more than 90% in 2 h. Geldanamycin also induced endocytosis of VEGFR1 in NIH3T3 cells transiently transfected with VEGFR1-GFP. Moreover, the geldanamycin-induced degradation of the endogenous VEGFR1 was evident in RAW cells. However, neither endocytosis (data not shown) nor protein degradation was observed in LDLR in the presence of geldanamycin.

To gain an insight into the mechanism of nLDL-induced degradation of VEGFR1, 3T3/VEGFR1 cells transfected with ubiquitin-Flag expression vectors were treated with VEGF, geldanamycin or nLDL. In all cases, the degradation of VEGFR1 was accompanied by ubiquitination of VEGFR1 (supplementary Fig 6A online). As the VEGF- or nLDL-induced degradation was

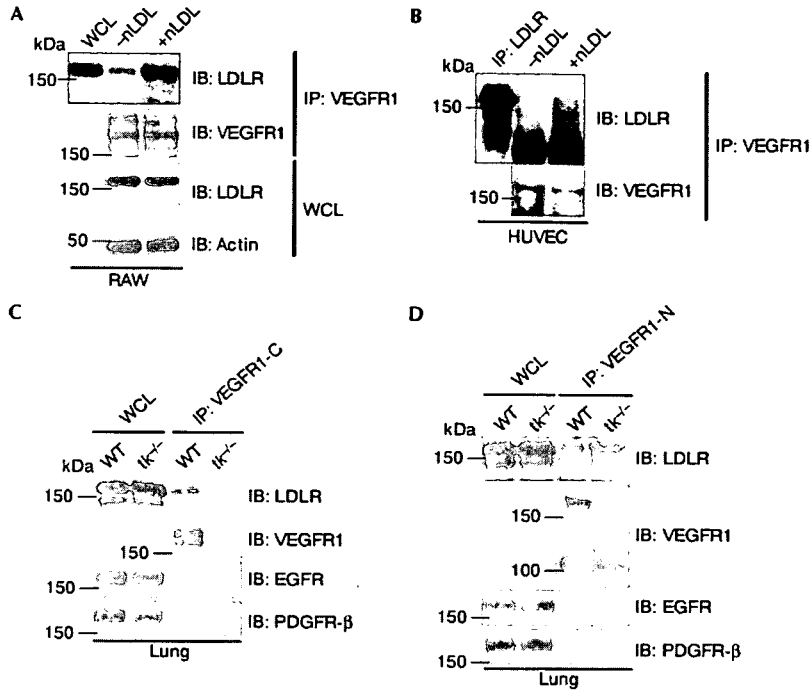

Fig 2 | Enhanced recruitment of the low-density lipoprotein receptor with VEGFR1 by native LDL stimulation. (**A**) Whole-cell lysates (WCLs) and anti-VEGFR1 immunoprecipitates (IP) from RAW cells, with (+nLDL) or without (−nLDL) stimulation by nLDL, were immunoblotted (IB) with LDLR, VEGFR1 and actin antibodies. (**B**) Anti-LDLR IP and anti-VEGFR1 IP from HUVEC, with (+nLDL) or without (−nLDL) stimulation by nLDL, were immunoblotted with LDLR or VEGFR1 antibody. (**C,D**) WCLs (60 μg each) and IPs by VEGFR (C) carboxy-terminal antibody (VEGFR1-C) or (D) amino-terminal antibody (VEGFR1-N) from lung lysates of WT or tk$^{-/-}$ mice were immunoblotted with LDLR, EGFR, PDGFR-β and the corresponding VEGFR1 antibody. EGFR, epidermal growth factor receptor; HUVEC, human umbilical vein endothelial cells; LDL, low-density lipoprotein; LDLR, LDL receptor; nLDL, native LDL; PDGFR, platelet-derived growth factor receptor; VEGFR, vascular endothelial growth factor receptor; WCL, whole-cell lysate; WT, wild type.

inhibited by MG132 or bafilomycin, both proteasomes and lysosomes could be the site for degradation (supplementary Fig 6B online).

Intriguingly, nLDL induced autophosphorylation of VEGFR1, but not VEGFR2, in 3T3 cells that overexpress either of the receptors (Fig 3A,B). The phosphorylation was similarly observed with both commercially available nLDL and nLDL freshly prepared from volunteers (data not shown). The minimum dose of nLDL required for VEGFR1 phosphorylation is 5–10 μg/ml (Fig 3C). VEGFR1 has the ability to bind heparin. To eliminate the possibility that VEGFR1 could be activated by nLDL bound to heparin, which might have been contaminated during the preparation of nLDL, heparinase treatment experiments were carried out. The result was negative (supplementary Fig 6C online). The intensity of the VEGFR1 autophosphorylation by nLDL was approximately 20–30% of that by VEGF. As VEGFR1 could be transphosphorylated by Src family tyrosine kinases, such as Fyn or Yes (Mary *et al*, 2002), when it is stimulated by VEGF, we pretreated the cells with the VEGFR inhibitor SU5416 or the Src inhibitor PP2. SU5416 suppressed VEGFR1 phosphorylation by nLDL or VEGF, but PP2 failed to do so (Fig 3A). Anti-LDLR short interfering RNA (siRNA) experiments were carried out to test the LDLR dependency for VEGFR1 activation. As shown in Fig 3D, knockdown of LDLR expression levels by more than 90% abrogated nLDL-induced VEGFR1 autophosphorylation and its degradation, whereas control RNAs did not. Therefore, we suppose that phosphorylation of VEGFR by nLDL is specific for VEGFR1 and mediated by LDLR. VEGFR1 has major autophosphorylation sites, such as Tyr1169, which is responsible for cell migration (Cunningham *et al*, 1997), and minor ones, such as Tyr 1333 that we have shown to be essential for receptor endocytosis with recruitment of the c-Cbl–CD2AP complex (Kobayashi *et al*, 2004). Both anti-phospholipase C γ and anti-c-Cbl immunoprecipitates from 3T3/VEGFR1 cells stimulated by nLDL contained autophosphorylated VEGFR1 (Fig 3E,F). These results indicate that nLDL and VEGF use the same molecular mechanism for endocytosis and protein degradation, and that nLDL might regulate some biological functions of VEGF.

nLDL accelerates macrophage migration through VEGFR1

As reported previously (Hara *et al*, 1992; Shibuya, 2006), peritoneal macrophage migration can be promoted by both VEGF and nLDL (Fig 4). To eliminate the possibility that commercially available nLDL might be oxidized to some extent and thus could stimulate expression of the chemokine MCP1 (also known as chemokine ligand 2 (CCL2); Berliner *et al*, 1992), we treated the cells with MCP1-blocking antibody. Cells stimulated by MCP1,

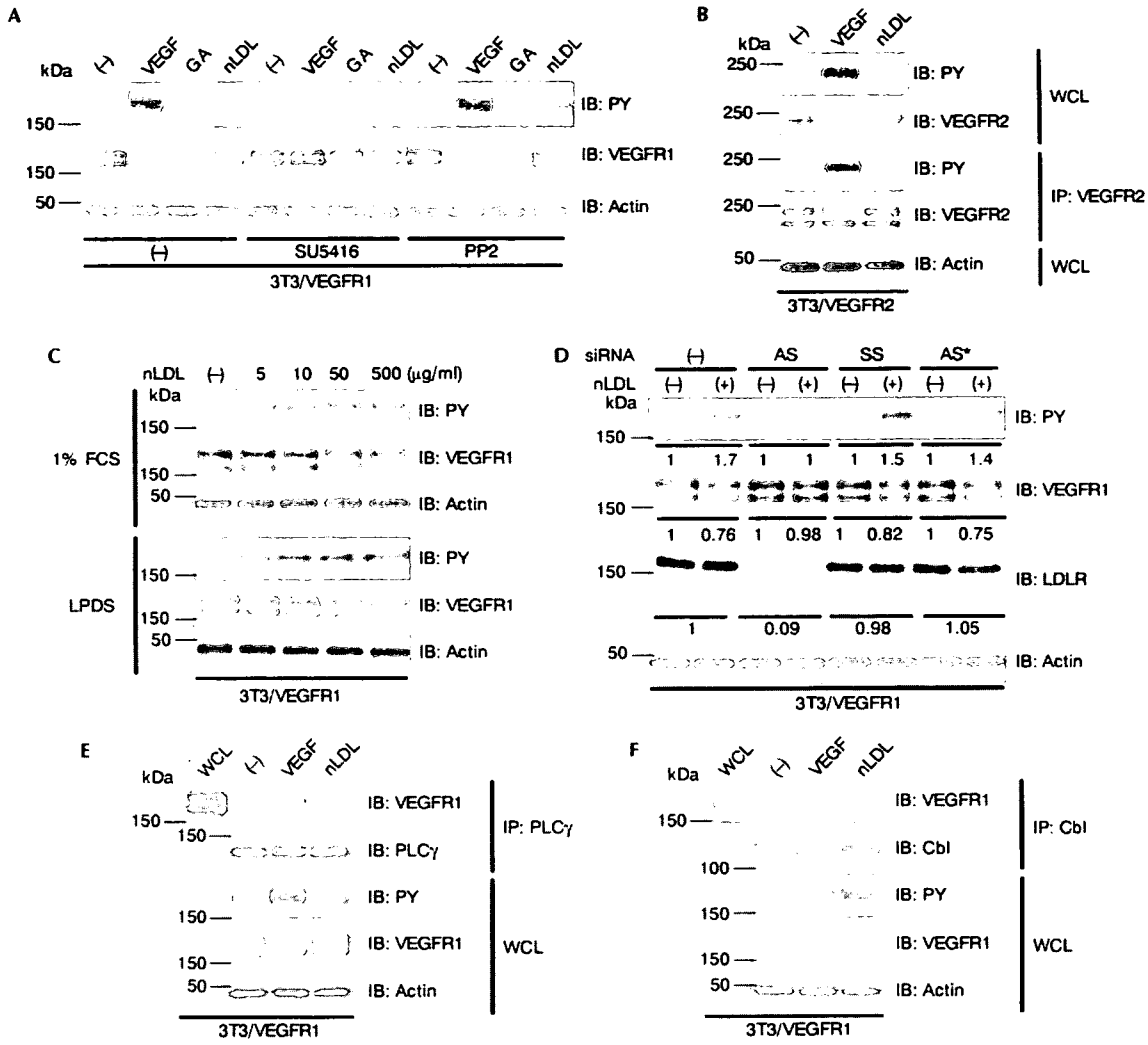

Fig 3 | Native low-density lipoprotein induces autophosphorylation of VEGFR1. (**A**) 3T3/VEGFR1 cells untreated (−) or pretreated with a VEGFR tyrosine kinase inhibitor SU5416 at 1 μM or Src inhibitor PP2 at 2 μM were stimulated by VEGF, GA or nLDL for 10 min. WCLs were immunoblotted (IB) with phosphotyrosine (PY), VEGFR1 and actin antibody. (**B**) WCLs or anti-VEGFR2 immunoprecipitates (IP) from 3T3/VEGFR2 cells stimulated with VEGF or nLDL were immunoblotted with PY, VEGFR2 and actin antibody. (**C**) WCLs from 3T3/VEGFR1 cells stimulated by the indicated concentration of nLDL after culture in 1% FCS or LPDS for 24 h were subjected to anti-PY, anti-VEGFR1 and anti-actin immunoblotting. (**D**) 3T3/VEGFR1 cells pretreated with mock (−), anti-LDLR siRNAs (antisense/sense: AS) or control siRNAs (sense/sense: SS or irrelevant siRNA against Nox1: AS*) at 40 nM were stimulated by nLDL for 10 min and then subjected to anti-PY, anti-VEGFR1, anti-LDLR and anti-actin immunoblotting. Relative average values of the band intensities from three independent experiments are shown below the western blot panels. (**E,F**) WCLs and (**E**) anti-PLCγ or (**F**) anti-c-Cbl IP from 3T3/VEGFR1 cells stimulated with VEGF or nLDL were immunoblotted with VEGFR1, PY, PLCγ (**E**), c-Cbl (**F**) and actin antibody. 3T3/VEGFR1, NIH3T3 cells that overexpress VEGFR1; GA, geldanamycin; LPDS, lipoprotein-deficient serum; nLDL, native LDL; PLC, phospholipase C; siRNA, short interfering RNA; VEGFR, vascular endothelial growth factor receptor; WCL, whole-cell lysate.

added to the culture, showed migrating ability that was blocked by the antibody. However, the antibody had no effect on the cells stimulated by nLDL (supplementary Fig 7 online). Interestingly, the nLDL-induced macrophage migration was repressed by SU5416 (Fig 4). This is consistent with the results shown in Fig 3E. The requirement for nLDL-induced migration by the tyrosine kinase activity of VEGFR1 was further confirmed by the inability of peritoneal macrophages from $tk^{-/-}$ mice to migrate. nLDL-induced migration was totally absent in macrophages from $LDLR^{-/-}$ mice, supporting our conclusion that nLDL activates VEGFR1 through LDLR.

DISCUSSION

The sorting proteins involved in LDLR endocytosis, such as autosomal recessive hypercholesterolaemia (ARH; Garuti *et al*, 2005), exert their function by binding to the NPXY motif found in

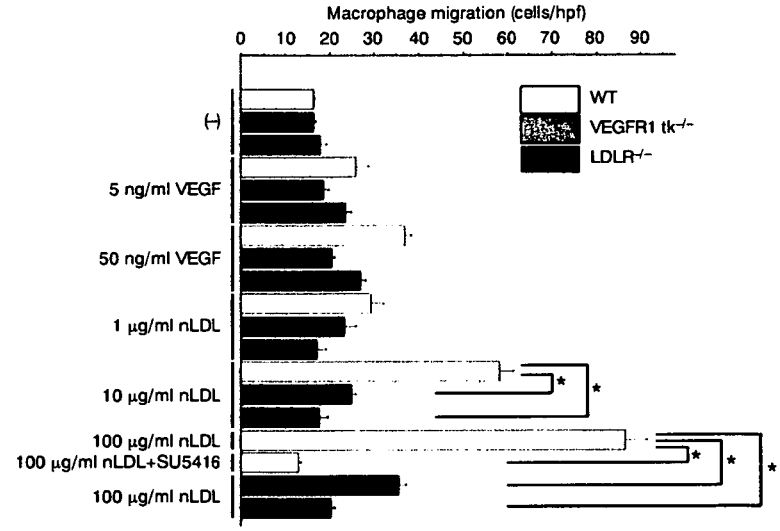

Fig 4 | Native low-density lipoprotein-induced macrophage migration is VEGFR1-dependent. VEGF or nLDL at the indicated concentrations was added to the lower chambers. Data were corrected for background intensities with no stimulation in WT mice and expressed as means ± s.d. $*P<0.001$. Assays were carried out in triplicate. hpf, high-power field; nLDL, native LDL; LDLR, LDL receptor; VEGFR, vascular endothelial growth factor receptor; WT, wild type.

the intracellular domain of LDLR. A mutation in the tyrosine residue within the motif abrogates receptor clustering in clathrin-coated pits. However, a recent study showed that LDLR can be internalized independently of this motif and dependently on the ligand very low density lipoprotein (VLDL) (Michaely *et al*, 2007). VEGFR1 has the conserved Tyr 1053 followed by NPD, which might act as the NPXY motif. Although Tyr 1053 is not a major autophosphorylation site in the detailed phosphotyrosine mapping analysis (Ito *et al*, 1998), the possibility that it is one of the minor sites cannot be completely excluded.

It still remains to be explained how VEGFR1 is activated by nLDL. Ligand-independent activation of receptor tyrosine kinase by another receptor is known in EGFR (Saito *et al*, 2001). In this case, platelet-derived growth factor (PDGF) transactivates EGFR in a superoxide-dependent or cytoplasmic Src tyrosine kinase-dependent manner with heterodimeric formation of PDGFR and EGFR. However, we repeatedly observed VEGFR1 activation and colocalization of LDLR and VEGFR1 even in the presence of PP2 or *N*-acetyl-cysteine (data not shown). Enzyme-linked immunosorbent assay of nLDL and fragment proteins containing the extracellular domain of VEGFR1 fused to the Fc portion of the immunoglobulin failed to prove direct binding between the two (data not shown). VEGF was not upregulated in nLDL-treated cells, thus negating the possibility of VEGFR1 activation by paracrine mechanisms. As the interaction of both receptors outside of the cells seems to be important for VEGFR1 activation by nLDL (Fig 2), we assume that nLDL-bound LDLR directly induces a conformational setting of VEGFR1 that might mimic the VEGF-bound and activated state.

VEGF expression is switched on and off depending on the biological circumstances, such as hypoxia, whereas nLDL is constantly and abundantly present in the serum. Given the VEGFR1 activation by nLDL in the absence of VEGF, our findings indicate that nLDL not only is the source of denatured LDL that activates scavenger receptors but also by itself could be a cause of atherosclerosis through VEGFR1.

METHODS

Molecular reagents. Antibodies and chemicals are listed in supplementary Table 1 online.

Plasmid construction. The GFP-tagged wild-type VEGFR1 expression vector has been described previously (Kobayashi *et al*, 2004). The full-length human LDLR complementary DNA was isolated from a human placenta cDNA library (Shibuya, 2006), sequenced and subcloned into pCMV-Tag4B expression vector.

Cell culture and transfections. NIH3T3 cells that overexpress VEGFR1 (3T3/VEGFR1) and VEGFR2 (3T3/VEGFR2) were described previously (Kobayashi *et al*, 2004). 293T, RAW264.7, CHO9 and NIH3T3 cells and skin fibroblasts isolated from wild-type and $LDLR^{-/-}$ mice were cultured in Dulbecco's modified Eagle's medium supplemented with 10% fetal calf serum. LPDS was prepared as described previously (Goldstein *et al*, 1983). The combination of transfection reagents, cells and primers for siRNA experiments are listed in supplementary Table 1 online.

Western blotting and immunoprecipitation analysis. 3T3/VEGFR1 cells cultured for 16–24 h in 1% FCS-containing DMEM were stimulated with 100 ng/ml VEGF or 500 μg/ml nLDL. Immunoprecipitation and western blotting were carried out as described previously (Okamoto *et al*, 2006) with the indicated antibodies (supplementary Table 1 online). For immunoprecipitation assay with lung lysates, 1% NP-40 was used instead of 1% Triton X-100. The intensity of bands in western blotting was quantified by Scion Image.

Immunofluorescence. 293T and RAW264.7, and CHO9 cells were transfected with VEGFR1-GFP and/or LDLR-Flag expression vectors. At 24 h after the transfection, the cells were starved of

serum for 8 h before being stimulated for 15 min at 37 °C with DiI-nLDL at 10 μg/ml, DiI-acLDL at 10 μg/ml, nLDL at 1, 10 or 100 μg/ml, or VEGF at 100 ng/ml. Peritoneal macrophages from mice were starved of serum for 24 h in 1% FCS before nLDL stimulation. They were then immunostained with the indicated antibody (supplementary Table 1 online) as described previously (Kobayashi *et al*, 2004). Fluorescent images were obtained by using Zeiss confocal laser scan microscopy (Zeiss, Oberkochen, Germany).

Ubiquitination assay. 3T3/VEGFR1 cells were transfected with a Flag-ubiquitin expression vector. At 24 h after transfection, the cells were treated with trypsin and replated to collagen-coated culture dishes with 1% FCS-containing media for 20 h. Cells stimulated by 100 ng/ml VEGF, 10 μM geldanamycin or 500 μg/ml nLDL were lysed in the ubiquitination assay buffer (50 mM NaCl, 10 mM Tris (pH 7.4), 5 mM EDTA, 50 mM NaF, 1% NP-40, 100 U/ml aprotinin, 10 mM *N*-ethylmaleimide and 50 μM LLnL).

Macrophage migration assay. The Boyden-chamber cell migration assay was carried out as described previously (Hiratsuka *et al*, 1998) with or without VEGF or nLDL at the indicated concentrations. In the statistical analyses, two-sided *P*-values of <0.05 were considered statistically significant.

Supplementary information is available at *EMBO reports* online (http://www.emboreports.org).

ACKNOWLEDGEMENTS

We thank B. Levene for correction of English in the manuscript. This study was partly supported by Grants-in-Aid for Scientific Research from the Japanese government (no. 12147210) to Y.M.

REFERENCES

Baigent C *et al*, Cholesterol Treatment Trialists' (CTT) Collaborators (2005) Efficacy and safety of cholesterol-lowering treatment: prospective meta-analysis of data from 90,056 participants in 14 randomised trials of statins. *Lancet* **366:** 1267–1278

Berliner JA, Territo M, Navab M, Andalibi A, Parhami F, Liao F, Kim J, Estworthy S, Lusis AJ, Fogelman AM (1992) Minimally modified lipoproteins in diabetes. *Diabetes* **41**(Suppl 2): 74–76

Brown MS, Goldstein JL (1986) A receptor-mediated passway for cholesterol homeostasis. *Science* **232:** 34–47

Crouse JR, Parks JS, Schey HM, Kahl FR (1985) Studies of low density lipoprotein molecular weight in human beings with coronary artery disease. *J Lipid Res* **26:** 566–574

Cunningham SA, Arrate MP, Brock TA, Waxham MN (1997) Interactions of FLT-1 and KDR with phospholipase Cγ: identification of the phosphotyrosine binding sites. *Biochem Biophys Res Commun* **240:** 635–639

Garuti R, Jones C, Li WP, Michaely P, Herz J, Gerard RD, Cohen JC, Hobbs HH (2005) The modular adaptor protein autosomal recessive hypercholesterolemia (ARH) promotes low density lipoprotein receptor clustering into clathrin-coated pits. *J Biol Chem* **280:** 40996–41004

Goldstein JL, Basu SK, Brown MS (1983) Receptor-mediated endocytosis of low-density lipoprotein in cultured cells. *Methods Enzymol* **98:** 241–260

Hara S, Nagano Y, Sasada M, Kita T (1992) Probucol pretreatment enhances the chemotaxis of mouse peritoneal macrophages. *Arterioscler Thromb* **12:** 593–600

Hiratsuka S, Minowa O, Kuno J, Noda T, Shibuya M (1998) Flt-1 lacking the tyrosine kinase domain is sufficient for normal development and angiogenesis in mice. *Proc Natl Acad Sci USA* **95:** 9349–9354

Ishibashi S, Goldstein JL, Brown MS, Herz J, Burns DK (1994) Massive xanthomatosis and atherosclerosis in cholesterol-fed low density lipoprotein receptor-negative mice. *J Clin Invest* **93:** 1885–1893

Ito N, Wernstedt C, Engstrom U, Claesson-Welsh L (1998) Identification of vascular endothelial growth factor receptor-1 tyrosine phosphorylation sites and binding of SH2 domain-containing molecules. *J Biol Chem* **273:** 23410–23418

Kobayashi S, Sawano A, Nojima Y, Shibuya M, Maru Y (2004) The c-Cbl/CD2AP complex regulates VEGF-induced endocytosis and degradation of Flt-1 (VEGFR-1). *FASEB J* **18:** 929–931

Lerdrup M, Hommelgaard AM, Grandal M, van Deurs B (2006) Geldanamycin stimulates internalization of ErbB2 in a proteasome-dependent way. *J Cell Sci* **119:** 85–95

Luttun A, Tjwa M, Moons L, Wu Y, Angelillo-Scherrer A, Liao F, Nagy JA, Hooper A, Priller J, De Klerck B (2002) Revascularization of ischemic tissues by PlGF treatment, and inhibition of tumor angiogenesis, arthritis and atherosclerosis by anti-Flt1. *Nat Med* **8:** 831–840

Mary TC, Jing W, Donald JF (2002) Src kinase becomes preferentially associated with the VEGFR, KDR/Flk-1, following VEGF stimulation of vascular endothelial cells. *BMC Biochem* **3:** 32

Matsumoto Y, Tanaka K, Hirata G, Hanada M, Matsuda S, Shuto T, Iwamoto Y (2002) Possible involvement of the vascular endothelial growth factor-Flt-1-focal adhesion kinase pathway in chemotaxis and the cell proliferation of osteoclast precursor cells in arthritic joints. *J Immunol* **168:** 5824–5831

Michaely P, Zhao Z, Wei-Ping Li, Garuti R, Huang LJ, Hobbs HH, Cohen JC (2007) Identification of a VLDL-induced, FDNPVY-independent internalization mechanism for the LDLR. *EMBO J* **26:** 3273–3282

Moore KJ, Freeman MW (2006) Scavenger receptors in atherosclerosis: beyond lipid uptake. *Arterioscler Thromb Vasc Biol* **26:** 1702–1711

Moulton KS, Vakili K, Zurakowski D, Soliman M, Butterfield C, Sylvin E, Lo KM, Gillies S, Javaherian K, Folkman J (2003) Inhibition of plaque neovascularization reduces macrophage accumulation and progression of advanced atherosclerosis. *Proc Natl Acad Sci USA* **100:** 4736–4741

Okamoto A, Iwamoto Y, Maru Y (2006) Oxidative stress-responsive transcription factor ATF3 potentially mediates diabetic angiopathy. *Mol Cell Biol* **26:** 1087–1097

Saito Y, Haendeler J, Hojo Y, Yamamoto K, Berk BC (2001) Receptor heterodimerization: essential mechanism for platelet-derived growth factor-induced epidermal growth factor receptor transactivation. *Mol Cell Biol* **21:** 6387–6394

Shibuya M (2006) Differential roles of vascular endothelial growth factor receptor-1 and receptor-2 in angiogenesis. *J Biochem Mol Biol* **39:** 469–478

Steinberg D, Parthasarathy S, Carew TE, Khoo JC, Witztum JL (1989) Beyond cholesterol. Modifications of low-density lipoprotein that increase its atherogenicity. *N Engl J Med* **320:** 915–924

SREBP-1-independent regulation of lipogenic gene expression in adipocytes

Motohiro Sekiya,* Naoya Yahagi,*,† Takashi Matsuzaka,§ Yoshinori Takeuchi,§ Yoshimi Nakagawa,§ Haruka Takahashi,* Hiroaki Okazaki,* Yoko Iizuka,* Ken Ohashi,* Takanari Gotoda,* Shun Ishibashi,* Ryozo Nagai,*,† Tsutomu Yamazaki,*,† Takashi Kadowaki,* Nobuhiro Yamada,§ Jun-ichi Osuga,* and Hitoshi Shimano[1,§]

Departments of Internal Medicine* and Clinical Bioinformatics,† Graduate School of Medicine, University of Tokyo, Tokyo 113-8655, Japan; and Advanced Biomedical Applications,§ Graduate School of Comprehensive Human Sciences, University of Tsukuba, Ibaraki 305-8575, Japan

Abstract **Sterol regulatory element-binding protein (SREBP)-1c is now well established as a key transcription factor for the regulation of lipogenic enzyme genes such as FAS in hepatocytes. Meanwhile, the mechanisms of lipogenic gene regulation in adipocytes remain unclear. Here, we demonstrate that those in adipocytes are independent of SREBP-1c. In adipocytes, unlike in hepatocytes, the stimulation of SREBP-1c expression by liver X receptor agonist does not accompany lipogenic gene upregulation, although nuclear SREBP-1c protein is concomitantly increased, indicating that the activation process of SREBP-1c by the cleavage system is intact in adipocytes. Supportively, transcriptional activity of the mature form of SREBP-1c for the FAS promoter was negligible when measured by reporter analysis. As an underlying mechanism, accessibility of SREBP-1c to the functional elements was involved, because chromatin immunoprecipitation assays revealed that SREBP-1c does not bind to the functional SRE/E-box site on the FAS promoter in adipocytes. Moreover, genetic disruption of SREBP-1 did not cause any changes in lipogenic gene expression in adipose tissue. In summary, in adipocytes, unlike in hepatocytes, increments in nuclear SREBP-1c are not accompanied by transactivation of lipogenic genes; thus, SREBP-1c is not committed to the regulation of lipogenesis.**—Sekiya, M., N. Yahagi, T. Matsuzaka, Y. Takeuchi, Y. Nakagawa, H. Takahashi, H. Okazaki, Y. Iizuka, K. Ohashi, T. Gotoda, S. Ishibashi, R. Nagai, T. Yamazaki, T. Kadowaki, N. Yamada, J-i. Osuga, and H. Shimano. **SREBP-1-independent regulation of lipogenic gene expression in adipocytes.** ***J. Lipid Res.*** **2007.** 48: **1581–1591.**

Supplementary key words sterol regulatory element-binding protein • lipogenesis • fatty acid synthase

The fatty acid biosynthetic pathway, composed of some 25 enzymes, has been elucidated in detail (1). Among these enzymes, FAS, the main synthetic enzyme that catalyzes the condensation of malonyl-CoA to produce the 16 carbon saturated fatty acid palmitate, and acetyl-coenzyme A carboxylase (ACC), which synthesizes malonyl-CoA from acetyl-CoA, are of particular importance. The regulation of these lipogenic enzymes has two remarkable features. First, their overall enzymatic activities largely depend on the amount of expressed protein that is primarily controlled at the transcriptional level, although regulation through phosphorylation is also important for some enzymes, such as ACC. Second, their rates of transcription are coordinately regulated (2). Therefore, it has been presumed that these genes share a regulatory sequence in their promoters that interacts with common *trans*-acting factors. In the liver, the most likely factor conducting this coordinated transcriptional regulation has been revealed to be sterol regulatory element-binding protein (SREBP)-1 (3, 4).

SREBPs are transcription factors that belong to the basic helix-loop-helix leucine zipper family and are considered to be profoundly involved in the transcriptional regulation of cholesterogenic and lipogenic enzymes (5, 6). Unlike other members of the basic helix-loop-helix leucine zipper family, SREBPs are synthesized as precursors bound to the endoplasmic reticulum and nuclear envelope. Upon activation, SREBPs are released from the membrane into the nucleus as mature protein by a sequential two-step cleavage process. To date, three SREBP isoforms, SREBP-1a, -1c, and -2, have been identified and characterized. SREBP-1a and -1c are transcribed from the same gene, each by a distinct promoter, and the predominant SREBP-1 isoform in liver and adipose tissue is 1c rather than 1a (7).

The role of SREBP-1c for the regulation of lipogenesis in the liver has been well established by several lines of

Manuscript received 10 August 2006 and in revised form 22 January 2007 and in re-revised form 12 April 2007.

Published, JLR Papers in Press, April 24, 2007.
DOI 10.1194/jlr.M700033-JLR200

Abbreviations: ACC, acetyl-coenzyme A carboxylase; ALLN, *N*-acetyl-leucyl-leucyl-norleucinal; ChIP, chromatin immunoprecipitation; LXR, liver X receptor; RXR, retinoid X receptor; SREBP, sterol regulatory element-binding protein.

[1]To whom correspondence should be addressed.
e-mail: shimano-tky@umin.ac.jp